Yuan *et al. Energy Mater* 2023;3:300032
DOI: 10.20517/energymater.2023.14

Energy Materials

Review

Open Access

Check for updates

The application of *in situ* liquid cell TEM in advanced battery research

Yi Yuan[1], Shengda D. Pu[1], Xiangwen Gao[2], Alex W. Robertson[3,*]

[1]Department of Materials, University of Oxford, Parks Road, Oxford OX1 3PH, UK.
[2]Future Battery Research Center, Global Institute of Future Technology, Shanghai Jiaotong University, Shanghai 200240, China.
[3]Department of Physics, University of Warwick, Coventry CV4 7AL, UK.

***Correspondence to:** Prof. Alex W. Robertson, Department of Physics, University of Warwick, Gibbet Hill Road, Coventry CV4 7AL, UK. E-mail: alex.w.robertson@warwick.ac.uk

How to cite this article: Yuan Y, Pu SD, Gao X, Robertson AW. The application of *in situ* liquid cell TEM in advanced battery research. *Energy Mater* 2023;3:300032. https://dx.doi.org/10.20517/energymater.2023.14

Received: 13 Mar 2023 **First Decision:** 21 Apr 2023 **Revised:** 12 May 2023 **Accepted:** 1 Jun 2023 **Published:** 5 Jul 2023

Academic Editor: Yizhong Huang **Copy Editor:** Fangling Lan **Production Editor:** Fangling Lan

Abstract

The fast development of modern battery research highly relies on advanced characterisation methods to unveil the fundamental mechanisms of their electrochemical processes. The continued development of *in situ* characterisation techniques allows the study of dynamic changes during battery cycling rather than just the initial and the final phase. Among these, *in situ* transmission electron microscopy (TEM) is able to provide direct observation of the structural and morphological evolution in batteries at the nanoscale. Using a compact liquid cell configuration, which allows a fluid to be safely imaged in the high vacuum of the TEM, permits the study of a wide range of candidate liquid electrolytes. In this review, the experimental setup is outlined and the important points for reliable operation are summarised, which are critical to the safety and reproducibility of experiments. Furthermore, the application of *in situ* liquid cell TEM in understanding various aspects, including dendrite growth, the solid electrolyte interface (SEI) formation, and the electrode structural evolution in different battery systems, is systematically presented. Finally, challenges in the current application and perspectives of the future development of the *in situ* liquid cell TEM technique are briefly addressed.

Keywords: *In situ* TEM, liquid cell electrochemical TEM, rechargeable batteries, dendrite growth, SEI formation

INTRODUCTION

The energy issue is one of the most concerning challenges facing society. Researchers have paid great efforts

to find alternative options to help us move beyond our heavy dependence on fossil fuels[1,2]. Batteries are considered a most promising alternative and have been rapidly developed to satisfy the fast-growing demands for electric vehicles, portable electrical devices, and other energy storage equipment in daily life[3,4]. Among all kinds of battery systems, the lithium (Li)-ion battery is at the forefront and has been extensively applied in various fields. More recently, many novel materials and battery systems have started to emerge as promising candidates, which may lead to higher capacity, lower cost, and safer operation[5-8].

Despite now achieving outstanding performance after decades of progress, Li-ion batteries are still facing significant challenges; one typical problem is that of dendritic growth[9,10], which is closely related to the unstable solid electrolyte interface (SEI) layer that forms across the electrodes, and directly leads to the degradation of batteries[11,12]. Therefore, it is an integral part of the current development of advanced batteries to explore the complicated degradation mechanisms that hinder their improvement.

Diverse characterisation techniques have been developed to understand the complicated reaction mechanisms in different battery systems[13-15] from aspects of anodes, cathodes, or their interfaces. Based on the different battery conditions during characterisation, these techniques can be broadly divided into two categories; *ex situ* methods that are performed "post-mortem" after cycling and *in situ* methods that are conducted during the cycling of a representative electrochemical cell. Typically, the *ex situ* methods are significantly easier in terms of sample preparation and requirements for equipment, but they can only give information about the initial and final states of batteries. However, the strength of *in situ* techniques is providing dynamic information in intermediate states, which brings more convenience to understanding the evolution of the electrodes and interfaces within working batteries. Furthermore, the dismantling of a cycled battery cell for *ex-situ* examination can cause misleading changes to the sample, such as due to air exposure or physical damage, which are avoided if the characterisation is done *in situ*.

A range of characterisation techniques has been adapted to testing environments in electrochemical cells, such as *in situ* X-ray diffraction (XRD)[16-20], *in situ* X-ray photoelectron spectroscopy (XPS)[21-23], *in situ* atomic force microscopy (AFM)[24-26], *in situ* X-ray computed tomography (CT)[27-30], *in situ* nuclear magnetic resonance (NMR)[31,32], *in situ* Fourier transform infrared spectroscopy (FTIR)[33,34], *in situ* Raman spectroscopy[35,36], differential electrochemical mass spectrometry (DEMS)[37-39], *in situ* optical microscopy (OM)[40,41], *in situ* scanning electron microscopy (SEM)[42,43], *in situ* transmission electron microscopy (TEM)[44-46], *etc*. These advanced *in situ* characterisation techniques have been independently or jointly applied to realise the analysis of the chemical components of SEI layers, the visualisation of electrode microstructures, and the exploration of chemical or electrochemical side reactions in electrolytes.

Among the above *in situ* characterisation methods, *in situ* TEM is a type of powerful technique that can capture the nanoscale morphological evolution and structural properties of electrode materials and the interfaces between electrodes and electrolytes. Compared with other *in situ* characterisation methods, such as the *in situ* OM, *in situ* CT, *in situ* AFM, *in situ* XRD, *etc*., the advantage of *in situ* TEM is that it can give structural and morphological information on the micro- to nano-level, with both better spatial and temporal resolutions than these other techniques. This, for instance, allows the identification of the initial nucleation stages of deposition processes, which usually is challenging to be observed by other techniques. A further advantage is that the mechanism for image contrast in TEM, which is sensitive to density/atomic number, can give compositional information to help with the analysis. In addition, it is also possible to conduct other *in situ* spectroscopic characterisations by using an electron beam.

There are two categories of *in situ* TEM, the open cell configuration and the closed cell configuration, as shown in Figure 1A and B. The *in situ* open cell TEM technique was initially used to observe Li dendrite formation. However, this open-cell investigation only allows the use of non-volatile electrolytes, either an ionic liquid or a solid electrolyte[47-52]. The *in situ* closed cell TEM, also known as *in situ* liquid cell TEM, has made it possible to monitor electrochemical dynamics and observe the growth of SEI and dendrites with more practical electrolytes[37,53-55]. As it is a sealed setup with liquids, gas evolution at the electrode/electrolyte interface can be detected by *in situ* liquid cell TEM experiments as well, which is of vital importance for investigating the properties of the SEI layer.

Herein, we present recent research progress in studying rechargeable batteries based on the application of *in situ* liquid cell TEM. First, we give a brief introduction to the experimental setup of the *in situ* liquid cell TEM and clarify several technical points that are worth taking into consideration during operation. Furthermore, observations on the growth of dendrites and SEI and other issues during cycling in Li, sodium (Na), zinc (Zn), magnesium (Mg), and calcium (Ca) electrolytes under *in situ* liquid cell TEM have been summarised, especially those results of Li batteries from aspects of electrolytes and electrode materials. Finally, we shed light on how we can better understand battery mechanisms with this technique in future research.

CONFIGURATION FOR IN SITU LIQUID CELL TEM HOLDER

The *in situ* liquid cell is prepared as a closed unit, in which silicon (Si) nitride membranes screen the liquid sample to prevent leakage of liquid electrolyte into the vacuum of the TEM while still allowing the electron beam to transmit through the cell and thus allow imaging of the sample. In the configuration of a typical commercial *in situ* liquid cell TEM holder, as shown in Figure 1C-E, inside the tip of the TEM holder, there is an electrical biasing Si chip and a sealing Si chip, as well as an O-ring, which helps these two chips to be aligned and sealed properly. The small Si chip is equipped with spacers of different heights at the edges or four corners, allowing the flow of liquids through the cell and accommodating electrochemical reactions on the electrode. Both Si chips have a window embedded in the centre, covered with an ultrathin, electron transparent layer, which is normally made of Si nitride (SiN_x) for most commercialised chips. Normally three electrodes are pre-patterned on the surface of a large chip, acting as a reference, working, and counter electrode. The tip of the working electrode, where reactions of interest occur, is patterned on the SiN_x window so it is visible by TEM.

As an aside, there is also another closed cell design named the graphene liquid cell (GLC), which uses graphene as the covering layer on the window[56]. However, it is not possible to apply biasing in the GLC for battery research so far, nor is it possible to replenish the limited cell volume by liquid flow, so it is not included in the scope of this review here.

EXPERIMENTAL SETUP FOR *IN SITU* LIQUID CELL TEM

The setup of *in situ* liquid cell TEM is very fragile, as the thickness of SiN_x membranes is normally around 50 nm. Improper handling during the experiment could result in blocking of the microfluidics or cell rupture and leakage, thus possibly causing detrimental or even fatal effects on the TEM column. This requires a thorough consideration of various factors when determining testing parameters in order to perform experiments safely without compromising too much on the imaging quality and desired information.

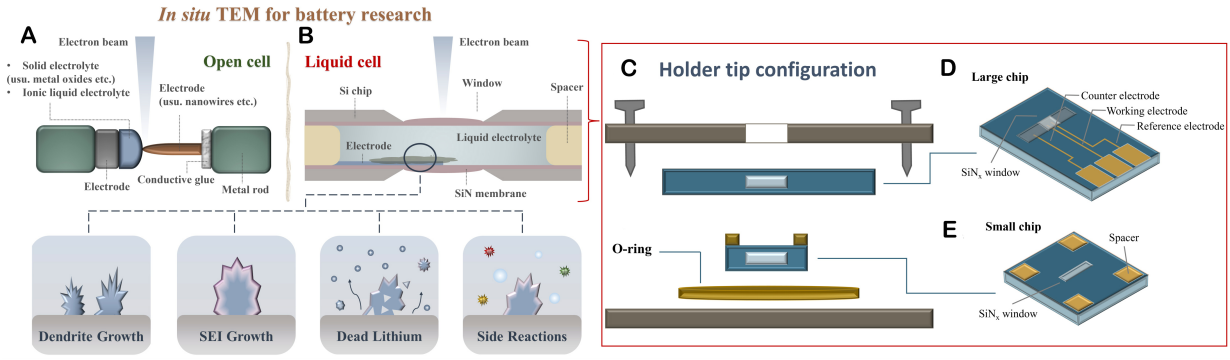

Figure 1. Schematics of *in situ* electrochemical TEM. A comparison of (A) the open cell and (B) the liquid cell approach for *in situ* electrochemical TEM experiments. (C) Cross-section view of the cell tip. (D) Typical electrode SiN and (E) sealing chips used to form the liquid cell.

Comprehensive studies of factors that determine the resolution of liquid cell TEM and scanning TEM (STEM) have been reported previously[57-60]. The resolution of the electron microscope is inversely proportional to the thickness of samples and directly proportional to the beam dose rate. This means a thinner liquid cell setup and higher dose rate can bring better resolution. However, a delicate balance between these factors and the resolution should be carefully monitored during imaging.

The total thickness of the *in situ* liquid cell setup comes from the sum of the thickness of SiN_x membranes and the thickness of the liquid. Normally, a thinner liquid layer is desired, although thicker liquid allows better diffusion of ions. Additionally, having more space within the cell chamber enables the observation of larger particles. However, it is important to note that the liquid thickness is constrained by the height of the spacers on the small chip, and it is not even. There will always be membrane bulging due to the pressure difference between the interior of the cell and the TEM column. As a result, the liquid is much thicker in the centre of the SiN_x window than at the edges. Thicker SiN_x membranes and smaller window sizes can help to eliminate the bulging, while this will compromise the resolution and field of view, respectively.

The beam dose rate is another factor that should be carefully controlled during imaging. Beam dose refers to the number of electrons that have irradiated a given area, usually with a unit of $e^- Å^{-2}$, while dose rate is defined as the dose in a unit of time, with a unit of $e^- Å^{-2} s^{-1}$. The accelerated electrons coming from the beam can inelastically interact with liquids, resulting in different types of beam damage, such as knock-on effect, thermal effect, radiolysis, *etc.*[57,58,61,62]. Systematic investigations into the impacts of beam damage on commonly used Li electrolytes were reported before[61]. Among them, radiolysis is the main concern that should be taken into consideration for liquid characterisation, especially for organic solvents, which can be less stable. It has been reported that radiolysis can cause the decomposition of liquids, resulting in changes in the local chemical environment and gas evolution[63-65]. This might give rise to misleading results of chemical properties and hinder the accurate acquisition of structural information. Therefore, it is necessary to conduct beam dose tests before performing *in situ* imaging and establish specific dose limits towards different samples experimentally. Related to beam dose control is the selection of an appropriate electron beam energy for the experiment. Typical electron beam energies used across TEM/STEM experiments are typically within the range of 60 kV to 300 kV, with 200 kV being the most frequently used. More recently, lower beam energies, such as 60 and 80 kV, have been used to study beam-sensitive 2D material-like graphene, as these are mainly susceptible to elastic (sputtering) damage from the electron beam, which is reduced for lower beam energies. However, for *in situ* liquid cell TEM, we need to ensure that (i) the beam transmits through the relatively thick liquid cell and (ii) that we minimise any beam damage. As discussed

above, the primary beam damage mechanism is via inelastic scattering for electrolyte studies, leading to radiolysis and charging, rather than elastic scattering, and so liquid cell studies are ideally performed with a high electron beam energy to ensure good beam transmission and minimise inelastic scattering.

The *in situ* liquid cell setup allows observation in either a static or a flowing state of solutions. The flow of liquids can be achieved by a syringe pump, of which the flowing rate is normally controlled at a μL/min level. As the cell and the syringe pump are usually connected by very fine channels, it is necessary to check the viscosity of the electrolyte to avoid any clogging. In terms of studies on batteries, a flowing liquid cell has several advantages. First, flowing fresh electrolytes into the small liquid cell can replenish the ions consumed during cycling, thus maintaining a consistent concentration of the electrolyte. Also, as discussed, most electrolytes are not so stable under the electron beam. In this case, a flowing electrolyte can help to refresh any potentially decomposed electrolytes induced by the beam, which may, otherwise, confuse the results.

Another point that should be taken into consideration is the choice of electrode materials on the chip. While the chip system is designed to imitate the target system as closely as possible, the electrode materials of chips are still limited. Typically, electrode materials used for chips include gold (Au), platinum (Pt), glassy carbon (GC), or titanium (Ti)[66,67]. An inappropriate base electrode material may interact with the electrolyte, potentially acting as an unwanted electrocatalyst for side reactions or undergoing alloying with electroplated material. Furthermore, the narrow gap and the extremely fragile membrane bring about more challenges to attaching desired materials to the chip. So far, several strategies for customising electrodes have been developed to accommodate various requirements for battery systems, including drop-casting[68,69], vacuum deposition[70], sample attachment via focused ion beam (FIB)[71], *etc*.

APPLICATION OF *IN SITU* LIQUID CELL TEM IN LI BATTERY SYSTEMS

To understand the complicated mechanisms occurring in battery systems, a variety of characterisation techniques have been developed over the past decades[13,72-75]. The *in situ* liquid cell TEM provides a powerful tool to explore the electrode materials and electrochemical reactions in batteries using liquid electrolytes, including the growth of dendrites, the formation of SEI layers, the changes to electrode structures, gas evolution, and more.

Li-ion batteries can now be found almost everywhere and are widely used in mobile phones, laptops, and electric vehicles, which have revolutionised our lives. Much progress has been made in improving the energy density, battery life, rapid charge, and safety of Li batteries in order to catch up with the increased demands of portable electronic devices and electric vehicles. Many attempts to develop various novel anode and cathode materials and advanced electrolyte systems have been reported to enhance the operating performance of Li batteries. However, one of the trickiest parts of addressing the above issues is to figure out the underlying causes for the degradation mechanisms of Li batteries during cycling.

In this section, progress on understanding the degradation mechanisms with the help of *in situ* liquid cell TEM in different Li battery systems will be summarised, and related studies targeted at electrolytes and electrode materials in Li batteries will be presented individually.

Electrolytes

Metallic Li is inherently thermodynamically unstable due to its chemical properties, and thus it can easily react with the majority of chemicals commonly used in liquid electrolyte systems, including salts, solvents, and additives[76-80]. The most commonly used salts include lithium hexafluorophosphate ($LiPF_6$), lithium

tetrafluoroborate ($LiBF_4$), lithium bis(oxalate)borate (LiBOB), lithium difluoro(oxalato)borate (LiDFOB), lithium bis(fluorosulfonyl)imide (LiFSI), lithium bis(trifluoromethanesulfonyl)imide (LiTFSI), lithium perchlorate ($LiClO_4$), *etc*., and the main solvents include propylene carbonate (PC), ethylene carbonate (EC), dimethyl carbonate (DMC), diethyl carbonate (DEC), dimethoxy sulfoxide (DMSO), and 1,2-dimethoxyethane (DME). This high activity of Li leads to severe instability of the anode/electrolyte interface, thus causing the problems of dendrite growth, SEI overgrowth, and dead Li accumulation. Therefore, investigating the interfacial evolution is of great significance as it can provide valuable insights and guide the search for possible solutions to improve the stability and cycling performance of Li batteries.

The properties of SEI layers on the electrode/electrolyte interface play a vital role in directing Li electrodeposition. There are several different models to describe the formation process of SEI layers, but the accurate formation process of complex SEI layers and the interaction between SEI layers and dendrites have not been fully revealed[11,12,81-84]. This exploration is partially limited by the characterisation techniques. Although various operando characterisation methods have been developed, it is still not feasible for most of them to provide direct observation of the electrode/electrolyte interfaces in a real battery working environment. For example, the *in situ* optical microscope can offer a real full-battery configuration but is unable to present structures at the micro level[40,41]. The *in situ* TEM open cell only allows the use of ionic liquids or solid electrolytes, and contact between the electrode and the electrolyte is usually limited to one spot, which could alter the diffusion of Li-ions, thus affecting the growth mechanisms of dendrites and SEI[85]. This illustrates the necessity of using the *in situ* liquid cell to capture the operando morphological evolution processes of Li dendrites and SEI in various electrolytes.

In 2014, the *in situ* evolution process of the electrode/electrolyte interface was directly captured by Zeng *et al*. using a homemade liquid cell chip with two electrodes and conducting cyclic voltammetry (CV) test [Figure 2A][86]. They observed inhomogeneous lithiation, lithium metal dendritic growth, electrolyte decomposition, and SEI formation on Au anodes from a commercial electrolyte of $LiPF_6$ in EC/DEC. The Li dendrites were found to nucleate and grow rapidly from the substrate. During the dissolution process, the stripping of dendrites started from the kink points and tip, leaving a branch-like structure on the substrate. Interestingly, bubbles formed due to the decomposition of the electrolyte solvent were also observed during the Li plating process. They also observed that the SEI layer was of equivalent thickness as previously reported, but they could not resolve the normally accepted two-layer structure, of which the inner layer is more compact with inorganic components while the outer layer is more porous.

A study was reported by Sacci *et al.* using similar CV cycling measurements, where they used a commercially available chip with a GC working electrode[87]. In the standard electrolyte of $LiPF_6$ in EC/DMC, they found that the formation of SEI dendrites began before Li deposition and that Li deposition occurred both beneath the SEI and also within the SEI, forming small crystalline particles [Figure 2B]. However, unlike normal dendritic morphologies, the Li electrodeposits in their images presented a more globular shape, and the secondary electrodeposits were a mixture of globular, faceted, and needle-like nucleation morphologies. This could possibly result from the involvement of carbon substrates or higher current densities. Mehdi *et al*. also reported the identification of Li dendrites and SEI on Pt electrodes in the electrolyte of $LiPF_6$ in PC[88]. They found Li plating on the Pt electrode was uniform; however, the dissolution of Li was not reversible. Li stripping left many dead Li around the electrode/electrolyte interface. The structural changes after extended cycling were also observed at the electrode, where a Li deposit formed underneath the SEI layer, and the SEI was found to crack due to the stresses of Li diffusion. Mehdi also presented a detailed discussion as to the expected contrast of lithium metal when observed in TEM or STEM; Li is darker than the background when imaged in dark-field mode, e.g., in the high-angle annular

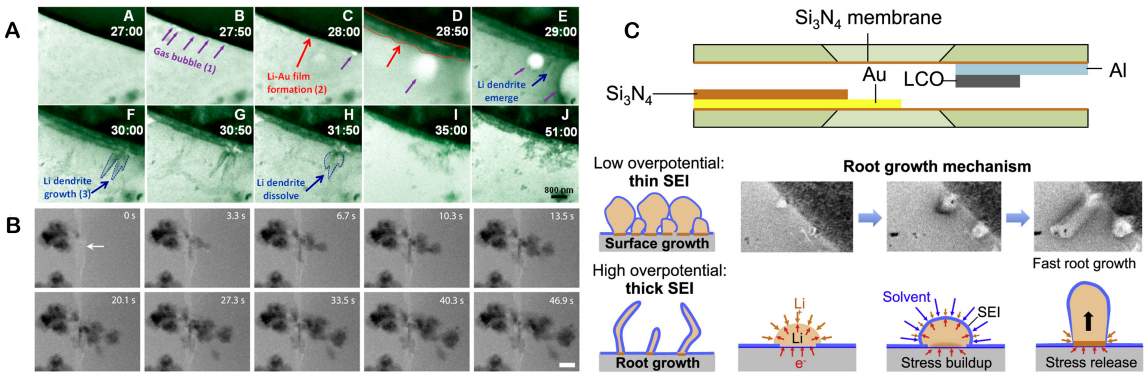

Figure 2. Electroplating and stripping of Li. (A) The evolving electrode-electrolyte interface of an Au electrode cycled in $LiPF_6$ EC/DMC electrolyte. Reproduced with permission[86]. Copyright 2014, American Chemical Society. (B) Li dendrite growth from $LiPF_6$ EC/DMC electrolyte. Lithium metal is dark contrast (bright field imaging). Scale bars are 1 μm. Reproduced with permission[87]. Copyright 2015, American Chemical Society. (C) Li deposition in a liquid cell with an application-relevant cathode material deposited on the counter electrode. Reproduced with permission[90]. Copyright 2017, Elsevier.

dark field (HAADF) STEM and brighter than the background in bright-field mode, e.g., conventional TEM. This is due to the density of lithium metal being lower than the surrounding electrolyte and the contrast of TEM being sensitive to the density.

Later, Li electrodeposition and dissolution on a Ti electrode in the standard electrolyte of $LiPF_6$ in EC/DMC was reported by Leenheer *et al.*[89]. They studied the influences of different cycling current densities in directing the morphologies of Li electrodeposits. Li deposits were compared under current densities of 1 mA/cm^2, 10 mA/cm^2, and 25 mA/cm^2. At the initial low current density, smooth deposition of large grains was seen. With the current increasing, needle-like crystals formed. They also reported the effects of electron irradiation on the Li morphologies, with faceted crystals and needles formed at 10 mA/cm^2 without beam exposure, while rounded nodules were found with beam exposure, illustrating the importance of accounting for the role of the electron beam in influencing these *in situ* experiments.

Apart from studying different dendrite and SEI morphologies, further research on exploring the nucleation mode and interaction of dendrites with SEI layers was conducted by Kushima[90]. They reported a comprehensive observation of lithium metal deposition and dissolution in the electrolyte of LiTFSI in DMSO. A customised chip with $LiCoO_2$ (LCO) film deposited on the counter electrode was studied [Figure 2C]. Li electrodeposition was first applied to investigate the Li growth mechanism in a liquid electrolyte. Electrolyte decomposition initially caused a thin SEI layer to coat the electrode. Then, Li nucleated over the electrode surface and grew, all beneath the SEI layer. Li was then observed to preferentially grow from existing root sites over the formation of new nucleation sites and was observed to also grow away from the root to form kinks in the dendrites due to the continually thickening SEI layer impeding ion transfer to the root. These types of complex, dynamically evolving growth dynamics can only be identified by direct nanoscale observation and are thus ideally suited to *in situ* liquid cell TEM.

Beyond these studies into the performance of standard Li electrolytes, other more novel electrolytes have been explored more recently, motivated by the desire to understand and improve the SEI. As has been shown in many battery studies, the properties of the SEI layers are determined by the electrolyte components. Therefore, seeking out proper electrolyte systems to enable SEI layers with high interfacial stability is an effective strategy to suppress Li dendrites and improve cycling performance. This is especially important for lithium metal batteries, where lithium metal is used as the anode material. Normally,

modifications of electrolyte systems are based on the consideration of several aspects, including the choice of proper solvents and salts, the concentration of the electrolyte, and the addition of extra additives. It is still not fully clear how the SEI layer structure and composition are controlled for these various electrolyte systems.

Electrolytes of high concentrations have been reported to be able to improve the properties of SEI layers, as there are much fewer free solvent molecules involved in reactions, leading to better cycle performance[91]. An electrolyte composed of 4M LiFSI in DME was demonstrated to provide a high coulombic efficiency over long-term cycling[92]. In addition, the morphology of Li electrodes cycled in coin cells was shown to be very uniform with dense columnar grains. To understand how this low-aspect-ratio structure formed, Harrison *et al.* performed observations of deposition behaviour in this high-concentration electrolyte[93]. Surprisingly, the coulombic efficiency was much lower, and the Li deposits did not exhibit the same morphologies previously observed in coin cells. In contrast, they found that there was a large amount of Li particles, and these particles were gradually consumed via self-discharge. They attributed this discrepancy to the compression in coin cells, which is hard to realise in the normal *in situ* liquid cell. This finding has indicated that mechanical cell compression is critical for building up stable SEI layers with dense and uniform structures.

Electrolyte additives have proven to be a powerful and feasible tool for modifying the SEI components. It is widely accepted that the LiF-rich SEI layers are helpful in suppressing Li dendritic growth and dead Li formation[94-97]. A lot of evidence has confirmed the role of LiF in establishing flat and dense SEI structures and monitoring Li deposit morphologies. Recently, Gong *et al.* demonstrated the direct imaging of the real-time dynamics of Li plating and stripping with the presence of the fluoroethylene carbonate (FEC) additive in $LiPF_6$ EC/DMC, as FEC is considered to promote the formation of fluoride-rich interphase[37]. They found the fluorinated system showed a denser deposition layer, where Li grains had better connectivity with each other than those without FEC. The better connection allowed complete striping as the Li maintained electric contact with the working electrode. The dynamic imaging showed it yielded a flatter and denser structure, thus also facilitating homogeneous ionic transport across the entire Li surface.

The effects of LiF-rich SEI layers were unveiled by Lee *et al.* as well via a well-designed *in situ* imaging setup[98]. They applied a poly(diallyldimethylammonium chloride) (PDDA) cationic polymer film on the liquid cell TEM electrode surface with the help of $Sn@SnO_2$ nanostructures (Sn nanowires/nanoparticles with a thin layer of surface oxide). As shown in Figure 3A, they observed Li nanogranule formation in the electrolyte of $LiPF_6$ in PC with the PDDA cationic polymer film, which normally arises from the LiF-rich SEI according to previous claims. The components of the LiF-rich SEI were confirmed by other elemental analyses. Unlike other strategies that directly supply extra fluorine in the electrolytes, the PDDA cationic polymer film was able to trap PF_6^- ions itself. The artificial uniformly distributed LiF-rich SEI layers were conducive to the nucleation of new Li nanogranules while suppressing further growth of existing Li deposits.

The stripping mechanisms of Li deposits were also studied recently, using the same experimental setup by this group[99]. It was found that the stripping processes of Li deposits with different morphologies obtained in the electrolyte of $LiPF_6$ in PC with and without PDDA coating can be described by one of the following three modes: (i) symmetric stripping; (ii) surface-preferred asymmetric stripping; and (iii) interface-preferred asymmetric stripping. These observations also confirmed that the formation of dead Li arose from the interface-preferred asymmetric stripping.

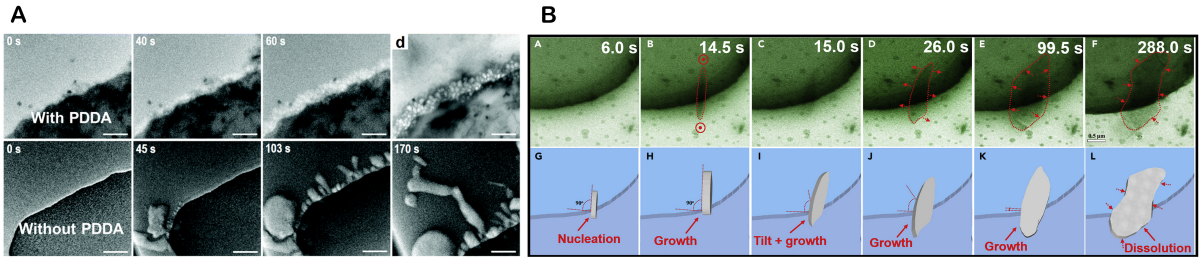

Figure 3. The influence of fluoride in Li electrochemical cycling. (A) Li plating with and without a fluoride-facilitating PDDA electrode coating. Reproduced with permission[98]. Scale bars are 1 μm. Copyright 2020, Royal Society of Chemistry. (B) Formation of a LiF nanocrystal from $LiPF_6$ in PC electrolyte. Reproduced with permission[55]. Copyright 2022, Cell Press.

Interestingly, the *in situ* formation of LiF nanocrystals was reported on positively charged Ti electrodes in the electrolyte of $LiPF_6$ in PC by Zhang *et al.* in their recent work[55]. The nucleation, growth, tilting, and dissolution of the LiF nanocrystals with a two-dimensional morphology are clearly shown in Figure 3B. The authors claimed that the observed LiF nanosheets on the positively charged Ti electrode could serve as a cathode electrolyte interface (CEI), which has not been reported in previous studies.

Electrode materials

In addition to the exploration of the Li dendrites and the SEI layers, *in situ* liquid cell TEM has also been applied to investigate morphological and structural changes of other electrode materials.

For novel anode materials for Li batteries, Si is considered one of the most promising candidates owing to its ultrahigh theoretical capacity (4,200 mA h g^{-1}), low working potential, and its high abundance in the Earth's crust[100]. However, Si anodes suffer from severe volume changes during the lithiation and delithiation process, which is over 300%[101]. The extreme expansion of Si anodes could lead to the pulverisation of active materials, the collapse of SEI layers and loss of electrical contact within the battery[102,103].

It has been proven that Si materials with nanostructures, such as nanowires and nanotubes, show the capability of easing the negative consequences of volume expansion[101,104]. What is more, appropriate surface coating to make it a core-shell structure has also turned out to be effective in strengthening the Si anode structure and increasing the electrical conductivity[105-107]. A lot of work has been done to investigate the degradation mechanisms of Si anode materials via *in situ* open cell TEM[108,109].

The lithiation behaviour of Cu-coated Si nanowires in the electrolyte of $LiClO_4$ in EC/DMC was first captured by Gu *et al.*[71]. Compared with previous *in situ* open cell research on Si anodes, one big advantage of the *in situ* liquid cell setup is to allow the immersion of the whole Si nanowire into the electrolyte instead of just a point contact. This helps to measure the volume expansion more accurately. As illustrated in Figure 4A, a single Si nanowire was mounted on the Pt electrodes by FIB manipulation and Pt deposition welding. The diameter of the Cu-coated Si nanowire was found to increase from 100 nm to 391 nm after lithiation, involving the anisotropic Si expansion and the SEI formation. Moreover, the rate of expansion was found to slow down with lithiation, which can be attributed to the interface stress limiting the Li diffusion into the core, in accordance with previous reports[108].

Later, Leenheer *et al.* further conducted direct observations of the lithiation mechanisms of amorphous Si, crystalline Al and crystalline Au using customised chips in the standard electrolyte of $LiPF_6$ in EC/DMC[110]. A homogeneous change in the contrast was observed during the lithiation/delithiation process of the

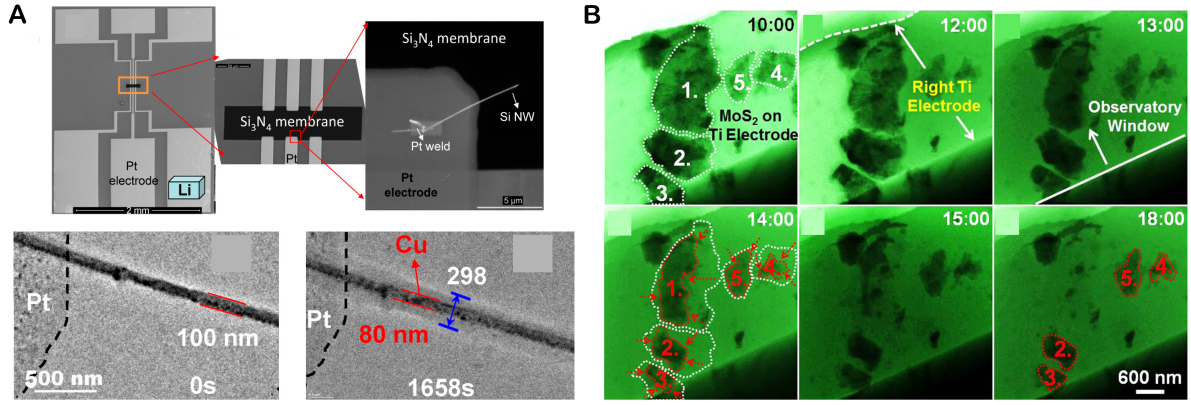

Figure 4. Lithiation of electrode materials. (A) Lithiation of a Si nanowire from $LiPF_6$ EC/DMC electrolyte. Reproduced with permission[71]. Copyright 2013, American Chemical Society. (B) Lithiation and delithiation of MoS_2 nanosheets on a Ti current collector from $LiPF_6$ EC/DEC electrolyte. Reproduced with permission[68]. Copyright 2015, American Chemical Society.

amorphous Si anode, corresponding to the uniform swelling and shrinking. However, there was insufficient contrast to visualise the two-stage mechanism, where Si will first turn into amorphous Li_xSi[109,111].

In addition, Zeng *et al.* also reported the observation of the lithiation/delithiation process of the layered MoS_2 nanosheets in an electrolyte of $LiPF_6$ in EC/DEC[68]. The MoS_2 nanosheets were successfully loaded on the Ti electrode via the simple drop-casting method. The MoS_2 nanosheets were found to undergo irreversible decomposition and fragmentation into nanoparticles in the voltage range of 1.8-1.2 V, as shown in Figure 4B.

Apart from anode materials, researchers have attempted to apply *in situ* liquid cell TEM to study cathode materials; however, this is more difficult than on interfaces and anode materials. There are significant structural transformations on the cathode side during the operation of the battery, such as the migration of transition metal atoms, the rearrangement of the metal-oxygen polyhedra, and the loss of oxygen in bulk or on the surface[112-116]. However, most of these structural changes happen at the unit cell level, which requires very high resolution to resolve. This cannot be easily captured with the presence of liquid electrolytes, which reduce the imaging resolution. Researchers are seeking out more advanced characterisation methods that can alleviate the effects of liquid electrolytes on imaging under the electron beam. Holtz *et al.* applied a type of spectroscopic imaging method that can visualise the microstructure and local electronic structure changes in the charging and discharging of electrode materials[117]. They used valence energy-filtered TEM (EFTEM) coupled with the electron energy-loss spectroscopy (EELS) and observed the lithiation and delithiation behaviour of the $LiFePO_4$ in the 0.5 M Li_2SO_4 aqueous electrolyte. Later, Karakulina *et al.* demonstrated structural changes of $LiFePO_4$ crystals at the unit cell level, which was achieved via the electron diffraction tomography (EDT) technique in the commercial liquid cell[69]. This technique is a viable alternative to *in situ* X-ray and neutron diffraction in terms of its advantage in locally characterising electrode crystals.

APPLICATION OF *IN SITU* LIQUID CELL TEM IN OTHER BATTERY SYSTEMS

In this section, the research on *in situ* liquid cell TEM goes beyond Li batteries. This includes investigations on Na batteries, Zn batteries, Mg batteries, Ca batteries, and progress on metal-air batteries. A brief summary of the findings in these areas will be provided.

Sodium batteries

As the second member of the alkali metal family, Na has been considered a competitive alternative energy storage material due to its similar properties to Li but much lower cost[118]. However, these similar chemical properties also induce the analogous uncontrollable dendrite problem. Recent studies have revealed some fundamental differences between Li and Na dendrites[119-122], which has drawn great attention to studying the in-depth mechanisms of Na dendrite growth. Various strategies have been implemented to suppress Na dendrites, among which the modification of the electrode structure is proven to be a highly effective method[119,122-125].

There has been some uncertainty in whether a uniform surface is necessary to overcome Na dendrites and what the potential consequences resulting from any unevenness will be. Zeng *et al.* reported their recent findings on the effects of electrode roughness on Na electrodeposition behaviour[126]. They patterned Ti electrodes with different curvatures on their homemade *in situ* liquid cell TEM chips, one with a flat surface and the other with a sharp tip. The differences in the nucleation and growth processes are shown in Figure 5A. On the flat Ti electrode, relatively large Na grains were observed at the edge of the electrode, along with gas bubbles emerging. In contrast, Na nodules were much smaller on the sharp Ti electrode [Figure 5B], and newly deposited Na was inclined to accumulate at the base of existing grains, indicating a "base growth" tendency, thus leading to an "explosive" growth behaviour. By characterising the SEI layers, the authors also claimed the thickness of SEI was playing a vital role in directing the growth rate and morphology of deposited Na.

Very recently, Gong *et al.* investigated the mechanisms of how ether-based electrolytes facilitate better cycling performance of Na battery anodes[53]. Under the *in situ* liquid cell TEM and HAADF-STEM imaging [Figure 6], severe gas evolution was observed in the carbonate electrolyte, while a similar phenomenon was not observed in the ether electrolyte. Further characterisations revealed that the enhanced elasticity of the ether-derived SEI played an important role in suppressing gas evolution and promoting uniform Na plating. This research also indicated the irreplaceable value of *in situ* liquid cell TEM in diagnosing battery reaction mechanisms.

Zinc batteries

The history of the Zn-based battery is nearly 200 years old, with the invention of Cu/Zn batteries by John Frederic Daniell in 1836[127]. Recently, the rechargeable Zn battery, using Zn metal as the anode, has been brought back to attention, primarily owing to the merits of high capacity and, in theory, low redox potential, low cost, and intrinsic safety, particularly due to the stability of Zn in aqueous solution[128,129]. However, similar to other metal anode materials, the metallic Zn also suffers from severe dendrite issues, which causes degradation of the battery performance[130-133]. Therefore, it is of vital importance to clarify the electrochemical deposition behaviour on the Zn anode.

The first observation of Zn deposition via *in situ* liquid cell TEM was reported by Park *et al.* in a ZnAu alloy system with Bi additives[134]. Later, the *in situ* nanoscale observations of pure Zn dendrites from $ZnSO_4$ aqueous electrolyte were reported by Sasaki *et al.*[70] and Li *et al.*[135], separately, in 2021. Li *et al.* demonstrated basic Zn deposition behaviour in the 0.3 M $ZnSO_4$ aqueous solution with the flow of electrolyte and compared differences in the dendrite formation at the nucleation stage and the growth stage under various applied currents and flow rates[135].

In the meantime, Sasaki *et al.* studied the Zn electrodeposition behaviour from diluted 0.1 M $ZnSO_4$ electrolytes in a static state[136]. The concentration of Zn^{2+} is equivalent to that of the 2.5 M KOH aqueous solution saturated with ZnO, which is widely used in rechargeable alkaline Zn batteries. This *in situ*

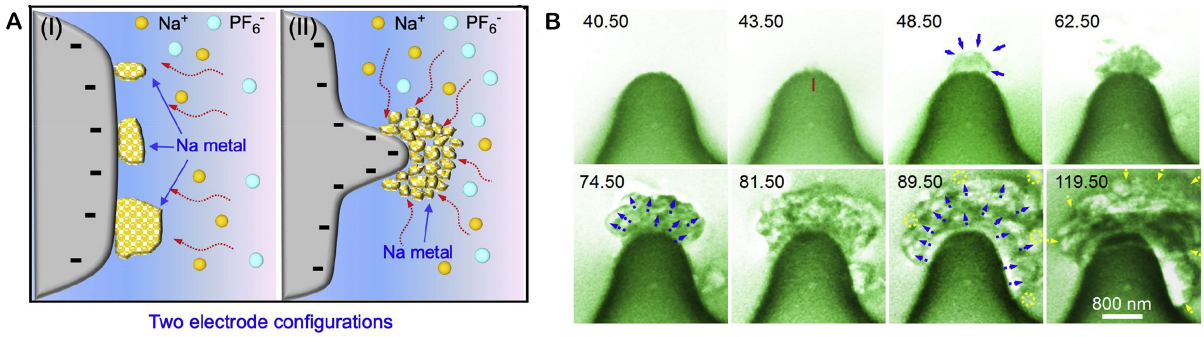

Figure 5. The influence of electrode roughness on Na electroplating. (A) A schematic illustrating the proposed influence of surface roughness on Na electrodeposition. (B) Liquid cell TEM imaging of Na plating on a sharp tip of the Ti current collector electrode. (A and B) Reproduced with permission[126]. Copyright 2020, Elsevier.

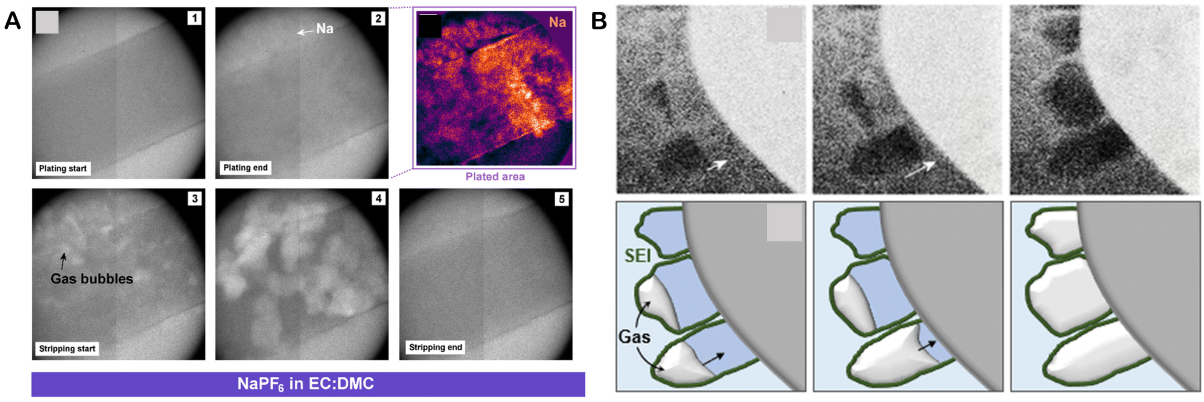

Figure 6. Gas evolution during Na electrostripping in the carbonate electrolyte. (A) Liquid cell TEM imaging of the Na plating and striping process. (B) Liquid cell HADDF-STEM imaging of the Na stripping process and corresponding cartoon illustrations. (A and B) Reproduced with permission[53]. Copyright 2023, Royal Society of Chemistry.

electrochemical experiment was conducted in a static electrolyte condition under a high current of 4 and 5 μA, equivalent to around 160 mA/cm^2 and 200 mA/cm^2 calculated from the active electrode surface area. What is more, to avoid gas generation at the counter electrode, they also coated a layer of Zn on the Pt counter electrode via vacuum deposition beforehand. Similar work was reported by this group later using the same experimental setup at lower current densities of 20 mA/cm^2 and 40 mA/cm^2 but with a modified potentiostat system that completely isolated the electrodes from the potential of the TEM column, achieving more reliable electrochemical data[136].

The evolution of Zn dendrites is shown in Figure 7A. Clear hexagonal Zn facets formed on the tip of the Pt electrode right after the electrochemical deposition started. With prolonged plating, needle-like Zn deposits were found to precipitate at the edge of the former facets, forming branch-like or seaweed-like structures at the end. A mechanism of such Zn dendrite formation was proposed by the authors, as given in Figure 7B. As Zn nuclei form and grow into larger hexagonal planar crystals, Zn-ions are consumed, and their concentration decreases from the centre of nucleation, resulting in a concentration gradient of Zn-ions surrounding the Zn deposits. This gradient favours nucleation and growth from the tips, which produces the branched Zn dendrites.

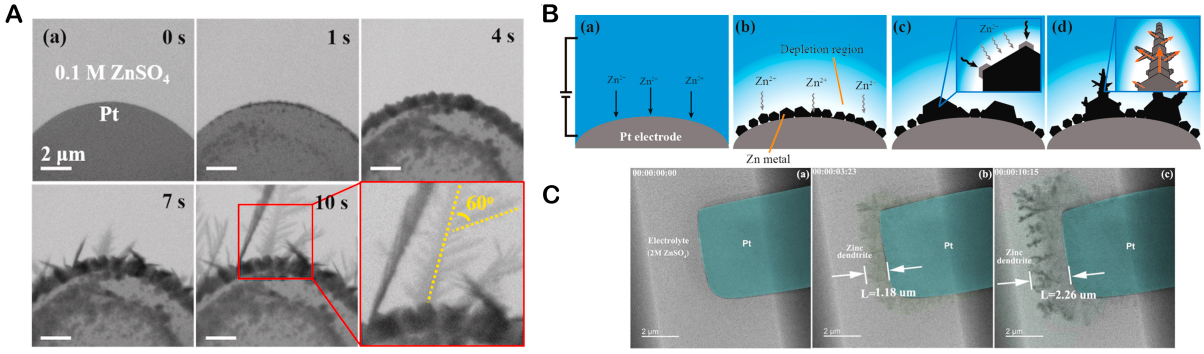

Figure 7. Zn dendrite formation. (A) Zn electrodeposition to a Pt working electrode from aqueous $ZnSO_4$ electrolyte. (B) Schematic illustrating the changing morphology as Zn deposition advanced. (A and B) Reproduced with permission[70]. Copyright 2021, Elsevier. (C) Electrostripping of deposited Zn dendrites, leaving behind isolated dead Zn. Reproduced with permission[137]. Copyright 2022, Elsevier.

Recently, Huang *et al.* further investigated the Zn plating/stripping and dendrite growth mechanisms in modified electrolyte systems[137]. They first presented a typical formation process of Zn dendrite and dead Zn in a wildly used 2 M $ZnSO_4$ mild aqueous electrolyte. The dendrite issue was verified, and a significant amount of dead Zn was observed left on the Pt electrode [Figure 7C].

$MnSO_4$ additive and the $Zn(CF_3SO_3)_2$ electrolyte have both been previously reported to be effective in optimising Zn ion batteries, of which the effects are generally considered to act on the cathode side[138-141]. To explore their effects on the Zn metal anode, dynamic Zn plating/stripping behaviours in the above two electrolytes were also studied. With Mn-ions in the electrolyte, nearly no dendrite-like Zn deposits were visible. Interestingly, some spherical particles were found to form and disintegrate around the Pt electrode during cycling. These particles were identified as insoluble Mn-based compounds triggered by the change in the pH value due to hydrogen (H_2) evolution. It was claimed by the authors that these spherical particles mechanically regulated the flow of ions and thus inhibited dendrite growth. As to the observation in the $Zn(CF_3SO_3)_2$ electrolyte, the Zn deposition was much more uniform and homogenous, and no obvious H_2 evolution happened, consistent with its superior performance in the coin cell test.

Magnesium batteries

Mg-ion batteries have gained wider research interest recently as one of the candidates for next-generation batteries[142-145]. This is primarily attributed to their ultrahigh theoretical volumetric capacity, as the Mg metal anode is of a volumetric capacity of 3,833 mAh cm^{-3} due to the divalent charge of the Mg-ion. Furthermore, Mg is also a non-toxic and earth-abundant element, which endows it with huge potential in future applications. Unlike Li batteries, Mg batteries are usually predicted to offer dendrite-free phases due to the higher potential to move Mg active species from the electrolyte bulk salt to the metal surface[146]. This prediction was verified by Wu *et al.* on both Ti and Au electrodes in the Magnesium Aluminium Chloride Complex (MACC) electrolyte, where $MgCl_2$ and $AlCl_3$ salts were dissolved in tetraethylene glycol dimethyl ether (TEGDME)[147]. From the *in situ* imaging evidence of Mg deposition [Figure 8A], it was found that a uniform Mg film was deposited on the electrode. This result has confirmed the intrinsic tendency of non-dendritic growth of Mg batteries, while this has turned out not to apply to all conditions in later studies[148-150].

Later, Singh *et al.* reported an observation of stable deposition and dissolution behaviour of Mg-ions in an electrolyte of Mg monocarborane (MMC) in tetraglyme (G4)[151]. Unlike previous TEM results, an SEI layer

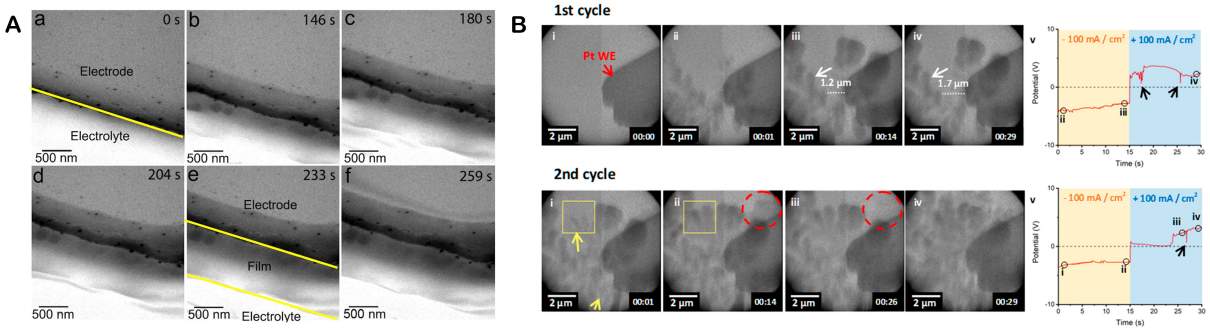

Figure 8. Mg and Ca electrodeposition. (A) Non-dendritic Mg electroplating. Reproduced with permission[147]. Copyright 2017, Springer Nature. (B) Ca dendrite formation from $Ca(BH_4)_2$ in THF electrolyte under high current density. Reproduced with permission[54]. Copyright 2020, American Chemical Society.

and unique Mg morphologies were discovered in the operando STEM analysis, which enabled continuous cycling without internal shorting. This stable SEI structure was claimed to be promising in the further practical application of metallic Mg anodes.

Calcium batteries

Ca batteries are also among the more promising future battery systems, with a relatively high theoretical capacity (2073 mAh cm^{-3}) and rich abundance on the Earth[152-154]. Recent progress in Ca electrolyte design has demonstrated the potential for Ca batteries to perform continuous cycling under mild conditions[155-157]. However, research on Ca batteries is still at a very initial stage, and the plating and stripping behaviour of Ca is still unclear. Recently, Pu *et al.* systematically studied the influence of the current density on the Ca plating/stripping processes in an electrolyte of 1M $Ca(BH_4)_2$ dissolved in tetrahydrofuran (THF)[54]. The morphologies of Ca deposits showed a high current-density dependence, as shown in Figure 8B, transforming from globular to dendritic shapes when the current was increased from 1 to 100 mA/cm^2. Interestingly, the sharp tips of Ca dendrites were found to expand into globular structures, as indicated in the yellow box. This "dendrite tip blunting" phenomenon potentially indicated a decrease in the local current density at the tips, which was suggested to be a consequence of the substantial increase in the plating surface area and the uneven charge distribution.

Metal-air batteries

Compared to the aforementioned metal-ion batteries, of which the energy storage is generated by the redox reaction of active transition metal oxides at the cathode, the metal-air batteries possess exceptionally high theoretical energy density, as they instead rely on cathode oxygen reduction with air harvested from the atmosphere[158-161]. This also endows them with ideal features, such as low cost and safety[162]. A series of metal-air battery systems have been developed, including Li[163,164], Na[165,166], K[167], Mg[168], Al[169], Zn[170,171], Fe[172], *etc.*

Li-O_2 batteries have been intensively studied over the past decades, which offer a theoretical energy density of 3,458 Wh/kg, based on the weight of the discharge product Li_2O_2[163,164]. However, the Li-O_2 batteries have suffered from a number of technical problems, such as limited practical energy efficiency[173], poor cycle life[174,175], low rate capability[176], and the noteworthy asymmetry between charging and discharging processes[164,177]. Various attempts have been made to diagnose the chemical mechanisms during discharging (the oxygen reduction reaction, ORR), charging (the oxygen evolution reaction, OER), and the origins of the severe parasitic reactions that occur[178-181].

Kushima *et al.* first reported the observation of the asymmetry in the morphological evolution of Li_2O_2 between charging and discharging in the electrolyte of LiTFSI in DMSO with the help of the *in situ* liquid cell TEM[182]. As shown in Figure 9A, the Li_2O_2 dendrites grew at the Li_2O_2/electrolyte interface in discharging while they decomposed from the root at the Li_2O_2/current collector interface. This tendency weakened the adhesion of Li_2O_2 to the current collector and reduced the contact area, contributing to the observed large overpotential. The detached insoluble Li_2O_2 fragments were also seen to be swept into the electrolyte upon minute flow agitations during cycling, which would be impossible to capture via traditional *ex situ* characterisation methods.

The problem of low practical capacity of the Li-O_2 batteries is closely related to the premature passivation of the air electrode caused by the formation of an insulating layer at the electrode, consisting of Li_2O_2 and other side reaction products[183,184]. Redox mediators are exploited to mitigate this problem, which can generate stable and soluble intermediate products, thus inducing the discharge process in the solution phase instead of on the electrode surface[185,186]. Several *in situ* qualitative and quantitative characterisation methods have been applied to reveal the roles of various redox mediators[179,187,188]. The effect of the redox mediator tetrathiafulvalene (TTF) in the electrolyte of 1 M $LiClO_4$ dissolved in DMSO was investigated via *in situ* liquid cell STEM by Yang *et al.*[189]. It was found that the TTF did not alleviate the formation of a solid Li_2O_2 phase during discharging, but it did function as an effective charge-transfer agent to promote the decomposition of the Li_2O_2 on charging. Later, Lee *et al.* reported the formation process of Li_2O_2 particles in the presence of 2,5-di-tert-butyl-1,4-benzoquinone (DBBQ) as the redox mediator[190]. It was directly observed that the Li_2O_2 particles formed in the solution phase via a two-step pathway. The particles first followed the lateral growth into a disclike shape and then grew vertically along the peripheral region, forming a toroidal morphology.

As mentioned above, the Li-O_2 system has intrinsic limitations in terms of efficiency due to parasitic reactions on the interfaces between the discharge product Li_2O_2 and both the electrode and the electrolyte[177,183]. Na-O_2 batteries are considered as a promising alternative due to better energy efficiency and presumably more limited side reactions, as the discharge product is normally Na superoxide (NaO_2), which is more stable[191,192]. Recently, Lutz *et al.* investigated the real-time nucleation and growth of NaO_2 in glyme-ether electrolytes for the first time[193]. As shown in Figure 9B, a solution-mediated nucleation process of the NaO_2 cubes was observed during reduction and the following oxidation process. It was identified that the growth process consisted of an initial incubation period (at 5 s), during which a cathodic current corresponding to the electrochemical formation of soluble NaO_2 was measured, but no product was seen on the electrode. This observation provided conclusive evidence that the NaO_2 did not follow the surface-directed growth. It was also found that a parasitic thick shell formed on the cube surface, isolating the NaO_2 cubes and passivating the electrode. This partially explained the reasons for the low efficiency during charge and the poor cyclability. It is worth mentioning here that the authors distinguished the thickness evolution of the parasitic shell via contrast filtering, which implied an efficient method to better analyse data obtained from *in situ* liquid cell TEM experiments.

CONCLUSION AND OUTLOOK

In situ liquid cell TEM occupies a unique role in allowing researchers to directly visualise nanoscale dynamic battery mechanisms that occur when cycling electrodes in liquid electrolytes, allowing for high spatial resolution, real-time imaging, high sensitivity contrast toward sample density, and the ability to study a wide range of candidate electrolytes. This combination of advantages is not currently achievable with any other technique. It has allowed for new perspectives into battery degradation behaviours, particularly in terms of our understanding of dendrite growth, SEI layer formation, and other

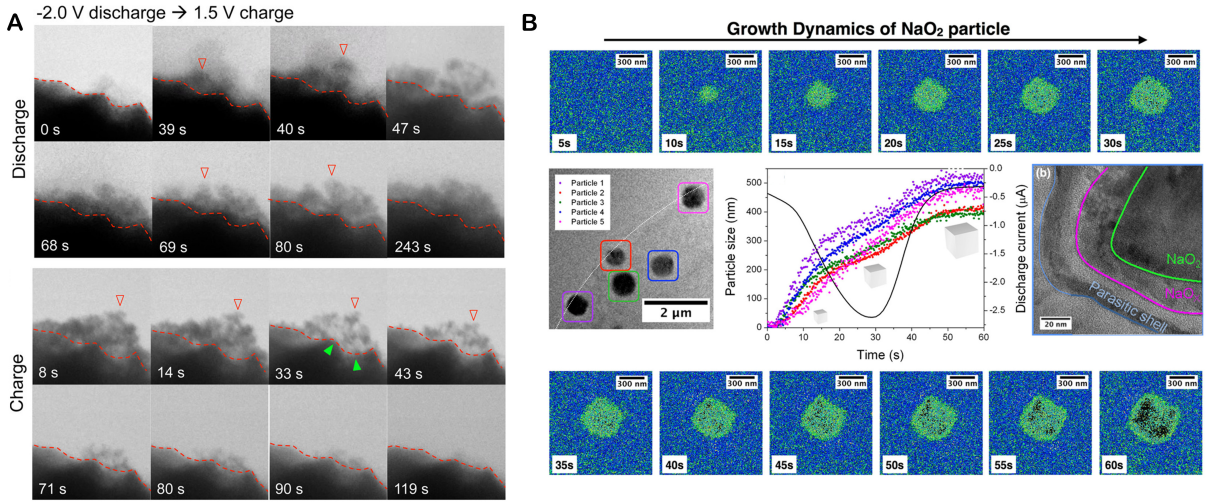

Figure 9. Understanding oxide formation for Li-O_2 and Na-O_2 batteries. (A) Li_2O_2 deposits forming and dissolving during cycling. Reproduced with permission[182]. Copyright 2015, American Chemical Society. (B) NaO_2 particle growth and nanocube formation. Reproduced with permission[193]. Copyright 2018, American Chemical Society.

electrochemical properties. Its ability to capture morphological and structural evolution endows researchers with a direct and straightforward tool to gain knowledge of the battery behaviours during cycling.

A practical challenge with liquid cell TEM experiments for studying battery materials is the difficulty in preparing suitable samples. The introduction of desired electrode materials on the chip is hindered by the fragile membranes and the technical difficulty in using compatible pre-deposition techniques. There are several approaches for preparing suitable chips, including controlled deposition via a nano-pipette from a scanning electrochemical cell microscope (SECCM), electrophoretic deposition from a suitable solution, or by functionalisation of the SiN window to make it "sticky" toward the target sample material[194,195]. Lithographic patterning and masking is another approach for ensuring that the target material only coats the working electrode and thus avoids the risks of short circuiting.

In addition to the challenges from the fabrication of the cell chips for *in situ* liquid cell TEM, there are also intrinsic limitations of liquid cell experiments. The correlation between the observed processes in the *in situ* TEM and the bulk battery performance is often difficult, as the electrochemical behaviours and mass transport are not equivalent due to very limited space within the liquid cell setup and thin-cell geometry[196,197]. As a result, the open circuit potential can be less stable than in conventional electrochemical cells, and the ionic concentration gradients may not be comparable either. The influence of the electron beam can also cause issues in collecting accurate electrochemistry, with the beam electrons undergoing elastic and inelastic interactions with the sample, with the latter scattering events generating low-energy secondary electrons that can go on to cause radiolysis, heating, and charging of the specimen. Therefore, electrochemical conditions within the liquid cell setup can be difficult to keep stable and reproducible for each reaction cycle, which makes obtained results less comparable to "lab bench" experiments. The high-energy electron beam can markedly alter the electrochemical behaviour and reaction kinetics of samples. For example, a recently published work systematically studied the effect of the electron beam on solid electrolytes by *in situ* open cell TEM, where delithiation of solid electrolytes was activated by a charging effect from the electron beam[198]. The issue of the confined sample volume and the influence of the beam make it challenging for the *in situ* liquid cell TEM technique to fully imitate the working conditions of real batteries.

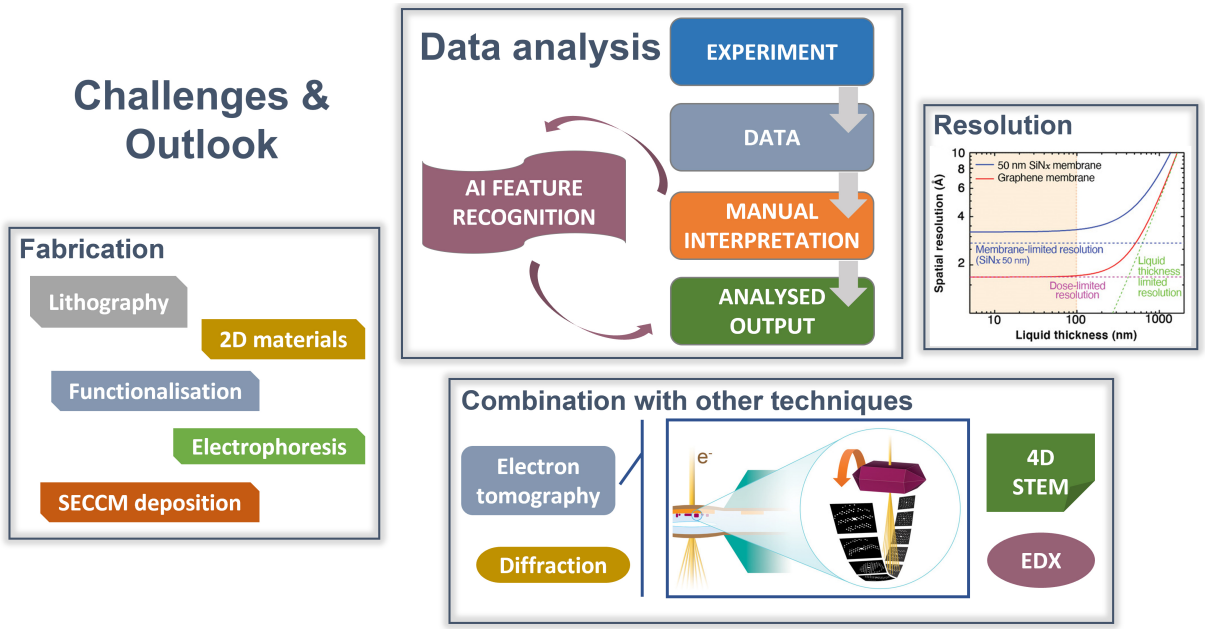

Figure 10. Current challenges and outlook of the future application of *in situ* liquid cell TEM. Reproduced with permission[69,199]. Copyright 2014, American Chemical Society.

Looking to the future, improving the imaging resolution of liquid-cell TEM is still of primary importance. One practical way is to reduce the thickness of the liquid cell and thereby reduce the scattering of the beam either by decreasing liquid layer thickness, reducing window thickness, or alleviating window bulging (Figure 10 - "Resolution"). For example, graphene-windowed environmental cells have been successfully designed, which could provide an atomic resolution if paired with a sufficiently thin liquid[199,200]. The use of low-dose imaging and/or controlled dose[201] and other advanced electron microscopy techniques, such as aberration correction TEM, pixelated detectors ("4D STEM"), or sub-sampling, can help to reduce the radiation damage and improve the image resolution and contrast. Beyond improving the spatial resolution, the future direction of *in situ* liquid cell TEM should aim to be more comprehensive, multifunctional, and cross-correlative. As discussed in the prior paragraph, new techniques for controllably mounting relevant electrode materials need to be devised to meet the demands of battery research of interest and devising ways of modifying the windows and/or electrode to facilitate higher resolution experiments (Figure 10 - "Fabrication")[194,195]. *In situ* liquid cell TEM should be integrated and correlated with other powerful complementary techniques, such as electron diffraction[69], X-ray spectroscopy[202,203], *etc.*, either using the same liquid cell setup or by other *ex situ* means (Figure 10 - "Combination with other techniques"). Advances in computational modelling and data analysis techniques will enable more efficient and effective analysis of the vast amounts of data generated by *in situ* TEM experiments (Figure 10 - "Data analysis")[204]. A significant problem across *in situ* characterisation is how to contend with the vast datasets that these techniques produce. Application of artificial intelligence (AI) tools to scour the collected data for correlations and features of interest would bypass the typical manual interpretation stage of experimental flow, which can be time-consuming and subjective, and would allow us to better handle these large datasets.

Based on continuing improvements in experimental and technical capabilities, in spite of these challenges, we believe the *in situ* liquid cell TEM will continue to play an important role in future battery research by providing insights into the dynamic behaviour of batteries under realistic operating conditions.

DECLARATIONS

Authors' contributions

Proposed the topic of this review and prepared the manuscript: Yuan Y, Robertson AW
Collectively discussed and revised the manuscript: Yuan Y, Pu SD, Gao X, Robertson AW

Availability of data and materials

Not applicable.

Financial support and sponsorship

None.

Conflicts of interest

All authors declared that there are no conflicts of interest.

Ethical approval and consent to participate

Not applicable.

Consent for publication

Not applicable.

REFERENCES

1. Davidson DJ. Exnovating for a renewable energy transition. *Nat Energy* 2019;4:254-6. DOI
2. Whittingham MS. History, evolution, and future status of energy storage. *Proc IEEE* 2012;100:1518-34. DOI
3. Kim H, Boysen DA, Newhouse JM, et al. Liquid metal batteries: past, present, and future. *Chem Rev* 2013;113:2075-99. DOI
4. Chao D, Zhou W, Xie F, et al. Roadmap for advanced aqueous batteries: From design of materials to applications. *Sci Adv* 2020;6:eaba4098. DOI PubMed PMC
5. Goodenough JB, Park KS. The Li-ion rechargeable battery: a perspective. *J Am Chem Soc* 2013;135:1167-76. DOI PubMed
6. Goodenough JB, Kim Y. Challenges for rechargeable Li batteries. *Chem Mater* 2010;22:587-603. DOI
7. Winter M, Barnett B, Xu K. Before Li ion batteries. *Chem Rev* 2018;118:11433-56. DOI PubMed
8. Etacheri V, Marom R, Elazari R, Salitra G, Aurbach D. Challenges in the development of advanced Li-ion batteries: a review. *Energy Environ Sci* 2011;4:3243-62. DOI
9. Gao X, Zhou Y, Han D, et al. Thermodynamic understanding of Li-dendrite formation. *Joule* 2020;4:1864-79. DOI
10. Zhang X, Wang A, Liu X, Luo J. Dendrites in lithium metal anodes: suppression, regulation, and elimination. *ACC Chem Res* 2019;52:3223-32. DOI
11. Peled E, Menkin S. Review - SEI: past, present and future. *J Electrochem Soc* 2017;164:A1703. DOI
12. Liu Q, Cresce A, Schroeder M, et al. Insight on lithium metal anode interphasial chemistry: reduction mechanism of cyclic ether solvent and SEI film formation. *Energy Stor Mater* 2019;17:366-73. DOI
13. Lu J, Wu T, Amine K. State-of-the-art characterization techniques for advanced lithium-ion batteries. *Nat Energy* 2017;2:17011. DOI
14. Lagadec MF, Zahn R, Wood V. Characterization and performance evaluation of lithium-ion battery separators. *Nat Energy* 2019;4:16-25. DOI
15. Atkins D, Ayerbe E, Benayad A, et al. Understanding battery interfaces by combined characterization and simulation approaches: challenges and perspectives. *Adv Energy Mater* 2022;12:2102687. DOI
16. Nazri G, Muller RH. In situ X-ray diffraction of surface layers on lithium in nonaqueous electrolyte. *J Electrochem Soc* 1985;132:1385. DOI
17. Balasubramanian M, Sun X, Yang X, Mcbreen J. In situ X-ray diffraction and X-ray absorption studies of high-rate lithium-ion batteries. *J Power Sources* 2001;92:1-8. DOI
18. Waluś S, Barchasz C, Colin JF, et al. New insight into the working mechanism of lithium-sulfur batteries: in situ and operando X-ray diffraction characterization. *Chem Commun* 2013;49:7899-901. DOI
19. Xia M, Liu T, Peng N, et al. Lab-scale in situ X-ray diffraction technique for different battery systems: designs, applications, and perspectives. *Small Methods* 2019;3:1900119. DOI

20. Guo JZ, Wang PF, Wu XL, et al. High-energy/power and low-temperature cathode for sodium-ion batteries: in situ XRD study and superior full-cell performance. *Adv Mater* 2017;29:1701968. DOI
21. Benayad A, Morales-Ugarte JE, Santini CC, Bouchet R. Operando XPS: a novel approach for probing the lithium/electrolyte interphase dynamic evolution. *J Phys Chem A* 2021;125:1069-81. DOI PubMed
22. Hikima K, Shimizu K, Kiuchi H, et al. Reaction mechanism of Li_2MnO_3 electrodes in an all-solid-state thin-film battery analyzed by operando hard X-ray photoelectron spectroscopy. *J Am Chem Soc* 2022;144:236-47. DOI
23. Shutthanandan V, Nandasiri M, Zheng J, et al. Applications of XPS in the characterization of battery materials. *J Electron Spectros Relat Phenomena* 2019;231:2-10. DOI
24. Zhang Z, Said S, Smith K, et al. Characterizing batteries by in situ electrochemical atomic force microscopy: a critical review. *Adv Energy Mater* 2021;11:2101518. DOI
25. Lang S, Shi Y, Hu X, Yan H, Wen R, Wan L. Recent progress in the application of in situ atomic force microscopy for rechargeable batteries. *Curr Opin Electrochem* 2019;17:134-42. DOI
26. Liu T, Lin L, Bi X, et al. In situ quantification of interphasial chemistry in Li-ion battery. *Nat Nanotechnol* 2019;14:50-6. DOI
27. Ning Z, Jolly DS, Li G, et al. Visualizing plating-induced cracking in lithium-anode solid-electrolyte cells. *Nat Mater* 2021;20:1121-9. DOI
28. Lu X, Bertei A, Finegan DP, et al. 3D microstructure design of lithium-ion battery electrodes assisted by X-ray nano-computed tomography and modelling. *Nat Commun* 2020;11:2079. DOI PubMed PMC
29. Jervis R, Kok MD, Neville TP, et al. In situ compression and X-ray computed tomography of flow battery electrodes. *J Energy Chem* 2018;27:1353-61. DOI
30. Kodama M, Komiyama S, Ohashi A, Horikawa N, Kawamura K, Hirai S. High-pressure in situ X-ray computed tomography and numerical simulation of sulfide solid electrolyte. *J Power Sources* 2020;462:228160. DOI
31. Bhattacharyya R, Key B, Chen H, Best AS, Hollenkamp AF, Grey CP. In situ NMR observation of the formation of metallic lithium microstructures in lithium batteries. *Nat Mater* 2010;9:504-10. DOI PubMed
32. Liu X, Liang Z, Xiang Y, et al. Solid-state NMR and MRI spectroscopy for Li/Na batteries: materials, interface, and in situ characterization. *Adv Mater* 2021;33:e2005878. DOI
33. Li J, Chen S, Ke F, Wei G, Huang L, Sun S. In situ microscope FTIR spectroscopic studies of interfacial reactions of Sn-Co alloy film anode of lithium ion battery. *J Electroanal Chem* 2010;649:171-6. DOI
34. Cheng H, Zhu C, Lu M, Yang Y. In situ micro-FTIR study of the solid-solid interface between lithium electrode and polymer electrolytes. *J Power Sources* 2007;174:1027-31. DOI
35. Cheng Q, Wei L, Liu Z, et al. Operando and three-dimensional visualization of anion depletion and lithium growth by stimulated Raman scattering microscopy. *Nat Commun* 2018;9:2942. DOI PubMed PMC
36. Xue L, Li Y, Hu A, et al. In situ/operando raman techniques in lithium-sulfur batteries. *Small Struct* 2022;3:2100170. DOI
37. Gong C, Pu SD, Gao X, et al. Revealing the role of fluoride-rich battery electrode interphases by operando transmission electron microscopy. *Adv Energy Mater* 2021;11:2003118. DOI
38. Zhu YG, Leverick G, Giordano L, et al. Nitrate-mediated four-electron oxygen reduction on metal oxides for lithium-oxygen batteries. *Joule* 2022;6:1887-903. DOI
39. Li F, Li ML, Wang HF, et al. Oxygen vacancy-mediated growth of amorphous discharge products toward an ultrawide band light-assisted Li-O_2 batteries. *Adv Mater* 2022;34:e2107826. DOI
40. Chen B, Zhang H, Xuan J, Offer GJ, Wang H. Seeing is believing: in situ/operando optical microscopy for probing electrochemical energy systems. *Adv Mater Technol* 2020;5:2000555. DOI
41. Merryweather AJ, Schnedermann C, Jacquet Q, Grey CP, Rao A. Operando optical tracking of single-particle ion dynamics in batteries. *Nature* 2021;594:522-8. DOI PubMed
42. Serra-Maia R, Kumar P, Meng AC, et al. Nanoscale chemical and structural analysis during in situ scanning/transmission electron microscopy in liquids. *ACS Nano* 2021;15:10228-40. DOI
43. Bülter H, Peters F, Schwenzel J, Wittstock G. Spatiotemporal changes of the solid electrolyte interphase in lithium-ion batteries detected by scanning electrochemical microscopy. *Angew Chem Int Ed* 2014;53:10531-5. DOI PubMed
44. Woods J, Bhattarai N, Chapagain P, Yang Y, Neupane S. In situ transmission electron microscopy observations of rechargeable lithium ion batteries. *Nano Energy* 2019;56:619-40. DOI
45. Zhang C, Firestein KL, Fernando JFS, Siriwardena D, von Treifeldt JE, Golberg D. Recent progress of in situ transmission electron microscopy for energy materials. *Adv Mater* 2020;32:e1904094. DOI PubMed
46. Fan Z, Zhang L, Baumann D, et al. In situ transmission electron microscopy for energy materials and devices. *Adv Mater* 2019;31:e1900608. DOI
47. Fahad S, Wei Z, Kushima A. In-situ TEM observation of fast and stable reaction of lithium polysulfide infiltrated carbon composite and its application as a lithium sulfur battery electrode for improved cycle lifetime. *J Power Sources* 2021;506:230175. DOI
48. Wen Y, Ding S, Ma C, et al. In situ TEM visualization of Ag catalysis in Li-O_2 nanobatteries. *Nano Res* 2023;16:6833-9. DOI
49. Wang K, Hua W, Huang X, et al. Synergy of cations in high entropy oxide lithium ion battery anode. *Nat Commun* 2023;14:1487. DOI PubMed PMC
50. Zhang Y, Zhao W, Kang C, et al. Phase-junction engineering triggered built-in electric field for fast-charging batteries operated at -30 °C. *Matter* 2023;6:1928-44. DOI

51. Ye W, Li X, Zhang B, et al. Superfast mass transport of Na/K via mesochannels for dendrite-free metal batteries. *Adv Mater* 2023;35:e2210447. DOI
52. Wang H, Liu F, Yu R, Wu J. Unraveling the reaction mechanisms of electrode materials for sodium-ion and potassium-ion batteries by in situ transmission electron microscopy. *Interdiscip Mater* 2022;1:196-212. DOI
53. Gong C, Pu SD, Zhang S, et al. The role of an elastic interphase in suppressing gas evolution and promoting uniform electroplating in sodium metal anodes. *Energy Environ Sci* 2023;16:535-45. DOI
54. Pu SD, Gong C, Gao X, et al. Current-density-dependent electroplating in Ca electrolytes: from globules to dendrites. *ACS Energy Lett* 2020;5:2283-90. DOI
55. Zhang Q, Ma J, Mei L, et al. In situ TEM visualization of LiF nanosheet formation on the cathode-electrolyte interphase (CEI) in liquid-electrolyte lithium-ion batteries. *Matter* 2022;5:1235-50. DOI
56. Park J, Koo K, Noh N, et al. Graphene liquid cell electron microscopy: progress, applications, and perspectives. *ACS Nano* 2021;15:288-308. DOI
57. de Jonge N, Houben L, Dunin-borkowski RE, Ross FM. Resolution and aberration correction in liquid cell transmission electron microscopy. *Nat Rev Mater* 2019;4:61-78. DOI
58. Pu S, Gong C, Robertson AW. Liquid cell transmission electron microscopy and its applications. *R Soc Open Sci* 2020;7:191204. DOI PubMed PMC
59. Gupta T, Schneider NM, Park JH, Steingart D, Ross FM. Spatially dependent dose rate in liquid cell transmission electron microscopy. *Nanoscale* 2018;10:7702-10. DOI PubMed
60. de Jonge N. Theory of the spatial resolution of (scanning) transmission electron microscopy in liquid water or ice layers. *Ultramicroscopy* 2018;187:113-25. DOI PubMed
61. Abellan P, Mehdi BL, Parent LR, et al. Probing the degradation mechanisms in electrolyte solutions for Li-ion batteries by in situ transmission electron microscopy. *Nano Lett* 2014;14:1293-9. DOI
62. Tao S, Li M, Lyu M, et al. In operando closed-cell transmission electron microscopy for rechargeable battery characterization: scientific breakthroughs and practical limitations. *Nano Energy* 2022;96:107083. DOI
63. Grogan JM, Schneider NM, Ross FM, Bau HH. Bubble and pattern formation in liquid induced by an electron beam. *Nano Lett* 2014;14:359-64. DOI PubMed
64. Lee J, Nicholls D, Browning ND, Mehdi BL. Controlling radiolysis chemistry on the nanoscale in liquid cell scanning transmission electron microscopy. *Phys Chem Chem Phys* 2021;23:17766-73. DOI PubMed
65. Schneider NM, Norton MM, Mendel BJ, Grogan JM, Ross FM, Bau HH. Electron-water interactions and implications for liquid cell electron microscopy. *J Phys Chem C* 2014;118:22373-82. DOI
66. Yang R, Mei L, Fan Y, et al. Fabrication of liquid cell for in situ transmission electron microscopy of electrochemical processes. *Nat Protoc* 2023;18:555-78. DOI
67. Sasaki Y, Mizushima A, Mita Y, Yoshida K, Kuwabara A, Ikuhara Y. Design and fabrication of an electrochemical chip for liquid-phase transmission electron microscopy. *Microscopy* 2022;71:238-41. DOI PubMed
68. Zeng Z, Zhang X, Bustillo K, et al. In situ study of lithiation and delithiation of MoS_2 nanosheets using electrochemical liquid cell transmission electron microscopy. *Nano Lett* 2015;15:5214-20. DOI
69. Karakulina OM, Demortière A, Dachraoui W, Abakumov AM, Hadermann J. In situ electron diffraction tomography using a liquid-electrochemical transmission electron microscopy cell for crystal structure determination of cathode materials for Li-ion batteries. *Nano Lett* 2018;18:6286-91. DOI PubMed
70. Sasaki Y, Yoshida K, Kawasaki T, Kuwabara A, Ukyo Y, Ikuhara Y. In situ electron microscopy analysis of electrochemical Zn deposition onto an electrode. *J Power Sources* 2021;481:228831. DOI
71. Gu M, Parent LR, Mehdi BL, et al. Demonstration of an electrochemical liquid cell for operando transmission electron microscopy observation of the lithiation/delithiation behavior of Si nanowire battery anodes. *Nano Lett* 2013;13:6106-12. DOI
72. Paul PP, Mcshane EJ, Colclasure AM, et al. A review of existing and emerging methods for lithium detection and characterization in Li-ion and Li-metal batteries. *Adv Energy Mater* 2021;11:2100372. DOI
73. Xu Y, Dong K, Jie Y, et al. Promoting mechanistic understanding of lithium deposition and solid-electrolyte interphase (SEI) formation using advanced characterization and simulation methods: recent progress, limitations, and future perspectives. *Adv Energy Mater* 2022;12:2200398. DOI
74. Liu X, Tong Y, Wu Y, Zheng J, Sun Y, Li H. In-depth mechanism understanding for potassium-ion batteries by electroanalytical methods and advanced in situ characterization techniques. *Small Methods* 2021;5:e2101130. DOI
75. Liu D, Shadike Z, Lin R, et al. Review of recent development of in situ/operando characterization techniques for lithium battery research. *Adv Mater* 2019;31:e1806620. DOI
76. Wang H, Yu Z, Kong X, et al. Liquid electrolyte: the nexus of practical lithium metal batteries. *Joule* 2022;6:588-616. DOI
77. Zhao C, Zhao B, Yan C, et al. Liquid phase therapy to solid electrolyte-electrode interface in solid-state Li metal batteries: a review. *Energy Stor Mater* 2020;24:75-84. DOI
78. Yang H, Li J, Sun Z, et al. Reliable liquid electrolytes for lithium metal batteries. *Energy Stor Mater* 2020;30:113-29. DOI
79. Eweka E, Owen J, Ritchie A. Electrolytes and additives for high efficiency lithium cycling. *J Power Sources* 1997;65:247-51. DOI
80. Lu Y, Tu Z, Shu J, Archer LA. Stable lithium electrodeposition in salt-reinforced electrolytes. *J Power Sources* 2015;279:413-8. DOI

81. Kong F, Kostecki R, Nadeau G, et al. In situ studies of SEI formation. *J Power Sources* 2001;97-8:58-66. DOI
82. Liu W, Liu P, Mitlin D. Review of emerging concepts in SEI analysis and artificial SEI membranes for lithium, sodium, and potassium metal battery anodes. *Adv Energy Mater* 2020;10:2002297. DOI
83. Zhai P, Liu L, Gu X, Wang T, Gong Y. Interface engineering for lithium metal anodes in liquid electrolyte. *Adv Energy Mater* 2020;10:2001257. DOI
84. Zhang X, Cheng X, Zhang Q. Advances in interfaces between Li metal anode and electrolyte. *Adv Mater Interfaces* 2018;5:1701097. DOI
85. Huang JY, Zhong L, Wang CM, et al. In situ observation of the electrochemical lithiation of a single SnO_2 nanowire electrode. *Science* 2010;330:1515-20. DOI PubMed
86. Zeng Z, Liang WI, Liao HG, Xin HL, Chu YH, Zheng H. Visualization of electrode-electrolyte interfaces in $LiPF_6$/EC/DEC electrolyte for lithium ion batteries via in situ TEM. *Nano Lett* 2014;14:1745-50. DOI PubMed
87. Sacci RL, Black JM, Balke N, Dudney NJ, More KL, Unocic RR. Nanoscale imaging of fundamental li battery chemistry: solid-electrolyte interphase formation and preferential growth of lithium metal nanoclusters. *Nano Lett* 2015;15:2011-8. DOI PubMed
88. Mehdi BL, Qian J, Nasybulin E, et al. Observation and quantification of nanoscale processes in lithium batteries by operando electrochemical (S)TEM. *Nano Lett* 2015;15:2168-73. DOI
89. Leenheer AJ, Jungjohann KL, Zavadil KR, Sullivan JP, Harris CT. Lithium electrodeposition dynamics in aprotic electrolyte observed in situ via transmission electron microscopy. *ACS Nano* 2015;9:4379-89. DOI PubMed
90. Kushima A, So KP, Su C, et al. Liquid cell transmission electron microscopy observation of lithium metal growth and dissolution: root growth, dead lithium and lithium flotsams. *Nano Energy* 2017;32:271-9. DOI
91. Jiang G, Li F, Wang H, et al. Perspective on high-concentration electrolytes for lithium metal batteries. *Small Struct* 2021;2:2000122. DOI
92. Qian J, Henderson WA, Xu W, et al. High rate and stable cycling of lithium metal anode. *Nat Commun* 2015;6:6362. DOI PubMed PMC
93. Harrison KL, Zavadil KR, Hahn NT, et al. Lithium self-discharge and its prevention: direct visualization through in situ electrochemical scanning transmission electron microscopy. *ACS Nano* 2017;11:11194-205. DOI
94. Zhao J, Liao L, Shi F, et al. Surface fluorination of reactive battery anode materials for enhanced stability. *J Am Chem Soc* 2017;139:11550-8. DOI
95. Cao X, Gao P, Ren X, et al. Effects of fluorinated solvents on electrolyte solvation structures and electrode/electrolyte interphases for lithium metal batteries. *Proc Natl Acad Sci USA* 2021;118:e2020357118. DOI PubMed PMC
96. Ko J, Yoon YS. Recent progress in LiF materials for safe lithium metal anode of rechargeable batteries: is LiF the key to commercializing Li metal batteries? *Ceram Int* 2019;45:30-49. DOI
97. Tan J, Matz J, Dong P, Shen J, Ye M. A growing appreciation for the role of LiF in the solid electrolyte interphase. *Adv Energy Mater* 2021;11:2100046. DOI
98. Lee S, Shangguan J, Alvarado J, et al. Unveiling the mechanisms of lithium dendrite suppression by cationic polymer film induced solid-electrolyte interphase modification. *Energy Environ Sci* 2020;13:1832-42. DOI
99. Lee S, Shangguan J, Betzler S, Harris SJ, Doeff MM, Zheng H. Lithium metal stripping mechanisms revealed through electrochemical liquid cell electron microscopy. *Nano Energy* 2022;102:107641. DOI
100. Sun L, Liu Y, Shao R, Wu J, Jiang R, Jin Z. Recent progress and future perspective on practical silicon anode-based lithium ion batteries. *Energy Stor Mater* 2022;46:482-502. DOI
101. Wu H, Cui Y. Designing nanostructured Si anodes for high energy lithium ion batteries. *Nano Today* 2012;7:414-29. DOI
102. Jin Y, Zhu B, Lu Z, Liu N, Zhu J. Challenges and recent progress in the development of Si anodes for lithium-ion battery. *Adv Energy Mater* 2017;7:1700715. DOI
103. Chae S, Ko M, Kim K, Ahn K, Cho J. Confronting issues of the practical implementation of Si anode in high-energy lithium-ion batteries. *Joule* 2017;1:47-60. DOI
104. Gonzalez A, Yang N, Liu R. Silicon anode design for lithium-ion batteries: progress and perspectives. *J Phys Chem C* 2017;121:27775-87. DOI
105. Yoshio M, Wang H, Fukuda K, Umeno T, Dimov N, Ogumi Z. Carbon-coated Si as a lithium-ion battery anode material. *J Electrochem Soc* 2002;149:A1598. DOI
106. Xu K, Liu X, Guan K, et al. Research progress on coating structure of silicon anode materials for lithium-ion batteries. *ChemSusChem* 2021;14:5135-60. DOI
107. Sim S, Oh P, Park S, Cho J. Critical thickness of SiO_2 coating layer on core@shell bulk@nanowire Si anode materials for Li-ion batteries. *Adv Mater* 2013;25:4498-503. DOI PubMed
108. Gu M, Li Y, Li X, et al. In situ TEM study of lithiation behavior of silicon nanoparticles attached to and embedded in a carbon matrix. *ACS Nano* 2012;6:8439-47. DOI
109. McDowell MT, Lee SW, Harris JT, et al. In situ TEM of two-phase lithiation of amorphous silicon nanospheres. *Nano Lett* 2013;13:758-64. DOI
110. Leenheer AJ, Jungjohann KL, Zavadil KR, Harris CT. Phase boundary propagation in Li-alloying battery electrodes revealed by liquid-cell transmission electron microscopy. *ACS Nano* 2016;10:5670-8. DOI PubMed
111. Wang CM, Li X, Wang Z, et al. In situ TEM investigation of congruent phase transition and structural evolution of nanostructured

silicon/carbon anode for lithium ion batteries. *Nano Lett* 2012;12:1624-32. DOI
112. Zhou H, Xin F, Pei B, Whittingham MS. What limits the capacity of layered oxide cathodes in lithium batteries? *ACS Energy Lett* 2019;4:1902-6. DOI
113. Liu X, Xu G, Kolluru VSC, et al. Origin and regulation of oxygen redox instability in high-voltage battery cathodes. *Nat Energy* 2022;7:808-17. DOI
114. Ding Z, Yang C, Zou J, et al. Reaction mechanism and structural evolution of fluorographite cathodes in solid-state K/Na/Li batteries. *Adv Mater* 2021;33:e2006118. DOI
115. House RA, Rees GJ, Pérez-osorio MA, et al. First-cycle voltage hysteresis in Li-rich 3D cathodes associated with molecular O_2 trapped in the bulk. *Nat Energy* 2020;5:777-85. DOI
116. House RA, Marie J, Pérez-osorio MA, Rees GJ, Boivin E, Bruce PG. The role of O_2 in O-redox cathodes for Li-ion batteries. *Nat Energy* 2021;6:781-9. DOI
117. Holtz ME, Yu Y, Gunceler D, et al. Nanoscale imaging of lithium ion distribution during in situ operation of battery electrode and electrolyte. *Nano Lett* 2014;14:1453-9. DOI
118. Delmas C. Sodium and sodium-ion batteries: 50 years of research. *Adv Energy Mater* 2018;8:1703137. DOI
119. Tian Z, Zou Y, Liu G, et al. Electrolyte solvation structure design for sodium ion batteries. *Adv Sci* 2022;9:e2201207. DOI PubMed PMC
120. Doi K, Yamada Y, Okoshi M, et al. Reversible sodium metal electrodes: is fluorine an essential interphasial component? *Angew Chem Int Ed* 2019;58:8024-8. DOI PubMed PMC
121. Ma L, Cui J, Yao S, et al. Dendrite-free lithium metal and sodium metal batteries. *Energy Stor Mater* 2020;27:522-54. DOI
122. Lee B, Paek E, Mitlin D, Lee SW. Sodium metal anodes: emerging solutions to dendrite growth. *Chem Rev* 2019;119:5416-60. DOI PubMed
123. Seh ZW, Sun J, Sun Y, Cui Y. A highly reversible room-temperature sodium metal anode. *ACS Cent Sci* 2015;1:449-55. DOI PubMed PMC
124. Bao C, Wang B, Liu P, et al. Solid electrolyte interphases on sodium metal anodes. *Adv Funct Mater* 2020;30:2004891. DOI
125. Xu M, Li Y, Ihsan-ul-haq M, et al. NaF-rich solid electrolyte interphase for dendrite-free sodium metal batteries. *Energy Stor Mater* 2022;44:477-86. DOI
126. Zeng Z, Barai P, Lee S, et al. Electrode roughness dependent electrodeposition of sodium at the nanoscale. *Nano Energy* 2020;72:104721. DOI
127. Shi Y, Chen Y, Shi L, et al. An overview and future perspectives of rechargeable zinc batteries. *Small* 2020;16:e2000730. DOI
128. Huy VP, Hieu LT, Hur J. Zn metal anodes for Zn-ion batteries in mild aqueous electrolytes: challenges and strategies. *Nanomaterials* 2021;11:2746. DOI PubMed PMC
129. Song M, Tan H, Chao D, Fan HJ. Recent advances in Zn-ion batteries. *Adv Funct Mater* 2018;28:1802564. DOI
130. Yang Q, Li Q, Liu Z, et al. Dendrites in Zn-based batteries. *Adv Mater* 2020;32:e2001854. DOI
131. Hao J, Li X, Zeng X, Li D, Mao J, Guo Z. Deeply understanding the Zn anode behaviour and corresponding improvement strategies in different aqueous Zn-based batteries. *Energy Environ Sci* 2020;13:3917-49. DOI
132. Hao J, Li B, Li X, et al. An in-depth study of Zn metal surface chemistry for advanced aqueous Zn-ion batteries. *Adv Mater* 2020;32:e2003021. DOI
133. Yi Z, Chen G, Hou F, Wang L, Liang J. Strategies for the stabilization of Zn metal anodes for Zn-ion batteries. *Adv Energy Mater* 2021;11:2003065. DOI
134. Park JH, Schneider NM, Steingart DA, Deligianni H, Kodambaka S, Ross FM. Control of growth front evolution by Bi additives during ZnAu electrodeposition. *Nano Lett* 2018;18:1093-8. DOI PubMed
135. Li M, Ran L, Knibbe R. Zn electrodeposition by an in situ electrochemical liquid phase transmission electron microscope. *J Phys Chem Lett* 2021;12:913-8. DOI
136. Sasaki Y, Yoshida K, Kuwabara A, Ikuhara Y. On-chip electrochemical analysis combined with liquid-phase electron microscopy of zinc deposition/dissolution. *J Electrochem Soc* 2021;168:112511. DOI
137. Huang Y, Gu Q, Guo Z, et al. Unraveling dynamical behaviors of zinc metal electrodes in aqueous electrolytes through an operando study. *Energy Stor Mater* 2022;46:243-51. DOI
138. Chamoun M, Brant WR, Tai C, Karlsson G, Noréus D. Rechargeability of aqueous sulfate Zn/MnO_2 batteries enhanced by accessible Mn^{2+} ions. *Energy Stor Mater* 2018;15:351-60. DOI
139. Wang F, Borodin O, Gao T, et al. Highly reversible zinc metal anode for aqueous batteries. *Nat Mater* 2018;17:543-9. DOI
140. Zhang N, Cheng F, Liu Y, et al. Cation-deficient spinel $ZnMn_2O_4$ cathode in $Zn(CF_3SO_3)_2$ electrolyte for rechargeable aqueous Zn-ion battery. *J Am Chem Soc* 2016;138:12894-901. DOI
141. Olbasa BW, Fenta FW, Chiu SF, et al. High-rate and long-cycle stability with a dendrite-free zinc anode in an aqueous Zn-ion battery using concentrated electrolytes. *ACS Appl Energy Mater* 2020;3:4499-508. DOI
142. Niu J, Zhang Z, Aurbach D. Alloy anode materials for rechargeable Mg ion batteries. *Adv Energy Mater* 2020;10:2000697. DOI
143. Asif M, Kilian S, Rashad M. Uncovering electrochemistries of rechargeable magnesium-ion batteries at low and high temperatures. *Energy Stor Mater* 2021;42:129-44. DOI
144. Mao M, Gao T, Hou S, Wang C. A critical review of cathodes for rechargeable Mg batteries. *Chem Soc Rev* 2018;47:8804-41. DOI
145. Shao Y, Gu M, Li X, et al. Highly reversible Mg insertion in nanostructured Bi for Mg ion batteries. *Nano Lett* 2014;14:255-60. DOI

146. Ling C, Banerjee D, Matsui M. Study of the electrochemical deposition of Mg in the atomic level: why it prefers the non-dendritic morphology. *Electrochim Acta* 2012;76:270-4. DOI
147. Wu YA, Yin Z, Farmand M, et al. In-situ multimodal imaging and spectroscopy of Mg electrodeposition at electrode-electrolyte interfaces. *Sci Rep* 2017;7:42527. DOI PubMed PMC
148. Kwak JH, Jeoun Y, Oh SH, et al. Operando visualization of morphological evolution in Mg metal anode: insight into dendrite suppression for stable Mg metal batteries. *ACS Energy Lett* 2022;7:162-70. DOI
149. Ding MS, Diemant T, Behm RJ, Passerini S, Giffin GA. Dendrite growth in Mg metal cells containing $Mg(TFSI)_2$/glyme electrolytes. *J Electrochem Soc* 2018;165:A1983. DOI
150. Davidson R, Verma A, Santos D, et al. Formation of magnesium dendrites during electrodeposition. *ACS Energy Lett* 2019;4:375-6. DOI
151. Singh N, Arthur TS, Tutusaus O, et al. Achieving high cycling rates via in situ generation of active nanocomposite metal anodes. *ACS Appl Energy Mater* 2018;1:4651-61. DOI
152. Lipson AL, Pan B, Lapidus SH, Liao C, Vaughey JT, Ingram BJ. Rechargeable Ca-ion batteries: a new energy storage system. *Chem Mater* 2015;27:8442-7. DOI
153. Nielson KV, Liu TL. Dawn of calcium batteries. *Angew Chem Int Ed* 2020;59:3368-70. DOI PubMed
154. Dompablo ME, Ponrouch A, Johansson P, Palacín MR. Achievements, challenges, and prospects of calcium batteries. *Chem Rev* 2020;120:6331-57. DOI PubMed
155. Nielson KV, Luo J, Liu TL. Optimizing calcium electrolytes by solvent manipulation for calcium batteries. *Batter Supercaps* 2020;3:766-72. DOI
156. Song H, Li Y, Tian F, Wang C. Electrolyte optimization and interphase regulation for significantly enhanced storage capability in Ca-metal batteries. *Adv Funct Mater* 2022;32:2200004. DOI
157. Li Z, Fuhr O, Fichtner M, Zhao-karger Z. Towards stable and efficient electrolytes for room-temperature rechargeable calcium batteries. *Energy Environ Sci* 2019;12:3496-501. DOI
158. Li L, Chang Z, Zhang X. Recent progress on the development of metal-air batteries. *Adv Sustain Syst* 2017;1:1700036. DOI
159. Sun Y, Liu X, Jiang Y, et al. Recent advances and challenges in divalent and multivalent metal electrodes for metal-air batteries. *J Mater Chem A* 2019;7:18183-208. DOI
160. Mei J, Liao T, Liang J, Qiao Y, Dou SX, Sun Z. Toward promising cathode catalysts for nonlithium metal-oxygen batteries. *Adv Energy Mater* 2020;10:1901997. DOI
161. Sharon D, Hirshberg D, Afri M, Frimer AA, Noked M, Aurbach D. Aprotic metal-oxygen batteries: recent findings and insights. *J Solid State Electrochem* 2017;21:1861-78. DOI
162. Wang H, Xu Q. Materials design for rechargeable metal-air batteries. *Matter* 2019;1:565-95. DOI
163. Liu T, Vivek JP, Zhao EW, Lei J, Garcia-Araez N, Grey CP. Current challenges and routes forward for nonaqueous lithium-air batteries. *Chem Rev* 2020;120:6558-625. DOI PubMed
164. Wang Y, Lu Y. Nonaqueous lithium-oxygen batteries: reaction mechanism and critical open questions. *Energy Stor Mater* 2020;28:235-46. DOI
165. Khan Z, Vagin M, Crispin X. Can hybrid Na-air batteries outperform nonaqueous Na-O_2 batteries? *Adv Sci* 2020;7:1902866. DOI PubMed PMC
166. Yadegari H, Sun X. Recent advances on sodium-oxygen batteries: a chemical perspective. *ACC Chem Res* 2018;51:1532-40. DOI PubMed
167. Park J, Hwang JY, Kwak WJ. Potassium-oxygen batteries: significance, challenges, and prospects. *J Phys Chem Lett* 2020;11:7849-56. DOI
168. Li C, Sun Y, Gebert F, Chou S. Current progress on rechargeable magnesium-air battery. *Adv Energy Mater* 2017;7:1700869. DOI
169. Ryu J, Park M, Cho J. Advanced technologies for high-energy aluminum-air batteries. *Adv Mater* 2019;31:e1804784. DOI PubMed
170. Yang D, Zhang L, Yan X, Yao X. Recent progress in oxygen electrocatalysts for zinc-air batteries. *Small Methods* 2017;1:1700209. DOI
171. Peng L, Shang L, Zhang T, Waterhouse GIN. Recent advances in the development of single-atom catalysts for oxygen electrocatalysis and zinc-air batteries. *Adv Energy Mater* 2020;10:2003018. DOI
172. Mckerracher RD, Ponce de leon C, Wills RGA, Shah AA, Walsh FC. A review of the iron-air secondary battery for energy storage. *ChemPlusChem* 2015;80:323-35. DOI
173. Débart A, Bao J, Armstrong G, Bruce PG. An O_2 cathode for rechargeable lithium batteries: the effect of a catalyst. *J Power Sources* 2007;174:1177-82. DOI
174. Débart A, Paterson AJ, Bao J, Bruce PG. Alpha-MnO_2 nanowires: a catalyst for the O_2 electrode in rechargeable lithium batteries. *Angew Chem Int Ed* 2008;47:4521-4. DOI PubMed
175. Bruce PG, Freunberger SA, Hardwick LJ, Tarascon JM. Li-O_2 and Li-S batteries with high energy storage. *Nat Mater* 2011;11:19-29. DOI PubMed
176. Zhang SS, Foster D, Read J. Discharge characteristic of a non-aqueous electrolyte Li/O_2 battery. *J Power Sources* 2010;195:1235-40. DOI
177. Peng Z, Freunberger SA, Hardwick LJ, et al. Oxygen reactions in a non-aqueous Li^+ electrolyte. *Angew Chem Int Ed* 2011;50:6351-5. DOI

178. Read J. Characterization of the lithium/oxygen organic electrolyte battery. *J Electrochem Soc* 2002;149:A1190. DOI
179. Schwager P, Bülter H, Plettenberg I, Wittstock G. Review of local in situ probing techniques for the interfaces of lithium-ion and lithium-oxygen batteries. *Energy Technol* 2016;4:1472-85. DOI
180. Zhu YG, Liu Q, Rong Y, et al. Proton enhanced dynamic battery chemistry for aprotic lithium-oxygen batteries. *Nat Commun* 2017;8:14308. DOI PubMed PMC
181. Mirzaeian M, Hall PJ. Characterizing capacity loss of lithium oxygen batteries by impedance spectroscopy. *J Power Sources* 2010;195:6817-24. DOI
182. Kushima A, Koido T, Fujiwara Y, Kuriyama N, Kusumi N, Li J. Charging/discharging nanomorphology asymmetry and rate-dependent capacity degradation in Li-oxygen battery. *Nano Lett* 2015;15:8260-5. DOI PubMed
183. Aurbach D, Mccloskey BD, Nazar LF, Bruce PG. Advances in understanding mechanisms underpinning lithium-air batteries. *Nat Energy* 2016;1:16128. DOI
184. Thotiyl MM, Freunberger SA, Peng Z, Bruce PG. The carbon electrode in nonaqueous Li-O_2 cells. *J Am Chem Soc* 2013;135:494-500. DOI
185. Chen Y, Freunberger SA, Peng Z, Fontaine O, Bruce PG. Charging a Li-O_2 battery using a redox mediator. *Nat Chem* 2013;5:489-94. DOI PubMed
186. Johnson L, Li C, Liu Z, et al. The role of LiO_2 solubility in O_2 reduction in aprotic solvents and its consequences for Li-O_2 batteries. *Nat Chem* 2014;6:1091-9. DOI
187. Yang K, Li Y, Jia L, et al. Atomic/nano-scale in-situ probing the shuttling effect of redox mediator in Na-O_2 batteries. *J Energy Chem* 2021;56:438-43. DOI
188. Ko Y, Kim H, Cho S, et al. Liquid-based janus electrolyte for sustainable redox mediation in lithium-oxygen batteries. *Adv Energy Mater* 2021;11:2102096. DOI
189. Yang C, Han J, Liu P, et al. Direct observations of the formation and redox-mediator-assisted decomposition of Li_2O_2 in a liquid-cell Li-O_2 microbattery by scanning transmission electron microscopy. *Adv Mater* 2017;29:1702752. DOI
190. Lee D, Park H, Ko Y, et al. Direct observation of redox mediator-assisted solution-phase discharging of Li-O_2 battery by liquid-phase transmission electron microscopy. *J Am Chem Soc* 2019;141:8047-52. DOI
191. Adelhelm P, Hartmann P, Bender CL, Busche M, Eufinger C, Janek J. From lithium to sodium: cell chemistry of room temperature sodium-air and sodium-sulfur batteries. *Beilstein J Nanotechnol* 2015;6:1016-55. DOI PubMed PMC
192. Hartmann P, Bender CL, Vračar M, et al. A rechargeable room-temperature sodium superoxide (NaO_2) battery. *Nat Mater* 2013;12:228-32. DOI
193. Lutz L, Dachraoui W, Demortière A, et al. Operando monitoring of the solution-mediated discharge and charge processes in a Na-O_2 battery using liquid-electrochemical transmission electron microscopy. *Nano Lett* 2018;18:1280-9. DOI
194. Tarnev T, Cychy S, Andronescu C, Muhler M, Schuhmann W, Chen YT. A universal nano-capillary based method of catalyst immobilization for liquid-cell transmission electron microscopy. *Angew Chem Int Ed* 2020;59:5586-90. DOI PubMed PMC
195. Robertson AW, Zhu G, Mehdi BL, Jacobs RMJ, De Yoreo J, Browning ND. Nanoparticle immobilization for controllable experiments in liquid-cell transmission electron microscopy. *ACS Appl Mater Interfaces* 2018;10:22801-8. DOI PubMed
196. Stricker EA, Ke X, Wainright JS, Unocic RR, Savinell RF. Current density distribution in electrochemical cells with small cell heights and coplanar thin electrodes as used in ec-S/TEM cell geometries. *J Electrochem Soc* 2019;166:H126. DOI
197. Zhang X, Liu W, Chen Z, Huang Y, Liu W, Yu Y. Pitfalls in electrochemical liquid cell transmission electron microscopy for dendrite observation. *Adv Energy Sustain Res* 2022;3:2100160. DOI
198. Peng X, Tu Q, Zhang Y, et al. Unraveling Li growth kinetics in solid electrolytes due to electron beam charging. *Sci Adv* 2023;9:eabq3285. DOI PubMed PMC
199. Koo K, Park J, Ji S, Toleukhanova S, Yuk JM. Liquid-flowing graphene chip-based high-resolution electron microscopy. *Adv Mater* 2021;33:e2005468. DOI PubMed
200. Dunn G, Adiga VP, Pham T, et al. Graphene-sealed flow cells for in situ transmission electron microscopy of liquid samples. *ACS Nano* 2020;14:9637-43. DOI
201. Stevens A, Yang H, Hao W, et al. Subsampled STEM-ptychography. *Appl Phys Lett* 2018;113:033104. DOI
202. Yang Y, Shao YT, Lu X, et al. Elucidating cathodic corrosion mechanisms with operando electrochemical transmission electron microscopy. *J Am Chem Soc* 2022;144:15698-708. DOI
203. Yang Y, Louisia S, Yu S, et al. Operando studies reveal active Cu nanograins for CO_2 electroreduction. *Nature* 2023;614:262-9. DOI
204. Spurgeon SR, Ophus C, Jones L, et al. Towards data-driven next-generation transmission electron microscopy. *Nat Mater* 2021;20:274-9. DOI PubMed PMC